Impact of Light Scatter on the Assessment of Retinal Arteriolar Hemodynamics

by

Behrooz Azizi

A thesis
presented to the University of Waterloo
in fulfillment of the
thesis requirement for the degree of
Master of Science
in
Vision Science

Waterloo, Ontario, Canada, 2010

Author's Declaration

I hereby declare that I am the sole author of this thesis. This is a true copy of the thesis, including any required final revisions, as accepted by my examiners.

I understand that my thesis may be made electronically available to the public.

Abstract

Introduction and Purpose:

Vascular pathologies play an important role in the etiology and progression of number of ocular diseases. Many instruments are developed to monitor retinal hemodynamics, including the Canon Laser Blood Flowmeter (CLBF), in an attempt to better understand the pathophysiology of the disease (Chapter 2). The purpose of this thesis is to determine the impact of light scatter on retinal arteriolar hemodynamic measurement assessed by the CLBF as intraocular light scatter is an inevitable consequence of ageing and particularly cataract.

Methodology:

Chapter 4 – Artificial light scatter model: One eye from each of 10 healthy young subjects between the ages of 18 and 30 (23.6 ± 3.4) was randomly selected. To simulate light scatter, cells comprising a plastic collar and two plano lenses were filled with solutions of differing concentrations of polystyrene microspheres (Polysciences Inc., USA). 0.002%, 0.004%, 0.006%, 0.008% were prepared, as well as distilled water only. After a preliminary screening to confirm subject eligibility, seven arteriolar hemodynamic measurements were taken by randomly placing the cells between the CLBF objective lens and the subjects' cornea.

Chapter 5 – Ten patients scheduled for extracapsular cataract extraction using phacoemulsification and intraocular lens implantation between the ages of 61 and 84 (mean age 73 years, SD ± 8) were prospectively recruited. Two visits were required to complete the study; One prior to the surgery and one at least six weeks after the surgery to allow for full post-operative recovery. The severity of cataract was documented using the Lens Opacity Classification System (LOCS, III) at the first visit. Each subject underwent visual function assessment at both visits using logMAR Early Treatment Diabetic Retinopathy Study (ETDRS) visual acuity charts and the Brightness Acuity Tester (BAT). Retinal arteriolar hemodynamics were measured at both visits using the high intensity setting of the Canon Laser Blood Flowmeter.

Results:

Chapter 4: Our light scatter model resulted in an artifactual increase of retinal arteriolar diameter ($p<0.0001$) and thereby increased retinal blood flow ($p<0.0001$). The 0.006% and 0.008% microsphere concentrations produced significantly higher diameter and flow values than baseline. Centerline blood velocity, however, was not affected by light scatter. Retinal arteriolar diameter values were significantly less with the high intensity laser than with the low intensity laser ($p=0.0007$).

Chapter 5: Group mean retinal arteriolar diameter and blood flow were reduced following extracapsular cataract extraction (Wilcoxon signed-rank test, $p=0.022$ and $p=0.028$ respectively); however, centerline blood velocity was unchanged (Wilcoxon signed-rank test, $p=0.074$).

Conclusions:

Using an artificial light scatter model (Chapter 3), we demonstrated that the densitometry assessment of vessel diameter is increasingly impacted as the magnitude of artificial light scatter increases; this effect can be partially negated by increasing laser intensity. We showed similar results in the presence of cataract (Chapter 4) by measuring the retinal arteriolar hemodynamics before and after removal of cataract. Care needs to be exercised in the interpretation of studies of retinal vessel diameter that use similar densitometry techniques as cataract is an inevitable consequence of aging.

Acknowledgements

I would like to express my sincere gratitude to my supervisor, Dr. Christopher Hudson, for his mentorship, patience, and support throughout my graduate studies. He was always a constant source of encouragement and hope.

I would also like to thank my thesis committee members Dr. John Flanagan and Dr. Natalie Hutchings for their support and helpful advice on my thesis work.

Sincere thanks to all my colleagues at the Retina Research Group, especially Tien Wong, Dr. Mila Kisilevsky, and Jennifer Wan for clinical assistance and helping me with the recruitments.

I would like to acknowledge the efforts of Dr. Singer at the University of Toronto and his staff, Jaala and Filomena, in recruiting patients. I would also like to thank Erin Harvey at the University of Waterloo for lending her invaluable expertise with the statistical analysis.

Dedication

I dedicate this work to my mother, Sheida. She is the most hard-working, loving, dedicated, selfless person I have ever known and I am blessed to have her in my life.

Table of Contents

Author's Declaration ..... *ii*

Abstract ..... *iii*

Acknowledgements ..... *v*

Dedication ..... *vi*

Table of Contents ..... *vii*

List of Figures ..... *ix*

List of Tables ..... *x*

1 Introduction *1*

1.1 Ocular Circulation **1**

1.2 Retinal Blood Flow **2**

1.2.1 Poiseuille's Law 2

1.2.2 Autoregulation of Blood Flow 2

1.2.3 Blood Flow and Ocular Diseases 3

1.3 Ocular Hemodynamic Assessment Techniques **3**

1.3.1 Pulsatility Measurement Devices 4

1.3.2 Angiography 4

1.3.3 Retinal vessel analyzer 5

1.3.4 Color Doppler Imaging 5

1.3.5 Laser Based Instruments 6

1.4 Cataract **11**

1.4.1 Optical Changes 11

1.4.2 Common Types of Cataract 12

1.4.3 Etiology of Cataract 13

1.4.4 Prevention & Management 15

1.4.5 Grading Cataract 16

1.5 Simulated Light Scatter Model **19**

1.6 Summary **19**

2 Rationale *21*

3 Impact of simulated light scatter on the CLBF *23*

3.1 Introduction **24**

3.2 Methods **25**

3.3 Results **30**

3.4 Discussion **34**

4 Assessment of Retinal Hemodynamics in Patients with Cataract 37

4.1 Introduction 38

4.2 Methods 39

4.3 Results 44

4.4 Discussion 47

5 Conclusions 49

References 51

Copyright Permission (Journal of Biomedical Optics) 60

Copyright Permission (Optometry Today) 61

Copyright Permission (Canon Inc., Japan) 62

List of Figures

Figure 1—1. Bidirectional laser Doppler Velocimetry. 7

Figure 1—2. Top Left: CLBF model 100, top right: operator's view showing the green laser locked on a branch of retinal vessel, bottom half: measurement window showing blood velocity curves and densitometry profile of the vessel diameter. 10

Figure 1—3. (a) contrast sensitivity function (CSF), (b) comparison of CSF for normal, refractive error and increased light scatter[68]. (Image reproduced by permission of OT, the magazine of the Association of Optometrists, www.optometry.co.uk) 17

Figure 3—1 Densitometry signal of a cross-sectional image acquired from a retinal arteriole. Min_1; minimum point in the central portion of the image designated as the nominal vessel center. D_1; signal level of Min_1 from the background level. D_2; signal level of the second minimum point in the neighborhood of Min_1. D_3 and D_4; signal levels of the maximum points on either side designated as the vessel edges. X_1 and X_2; the half height points whose signal levels are $(D_1+D_3)/2$ and $(D_2+D_4)/2$, respectively. The width between X_1 and X_2 is taken to represent the uncorrected vessel diameter. (Image courtesy of Canon Inc, Japan) 27

Figure 3—2 Change in retinal arteriolar diameter (upper), centerline blood velocity (middle) and blood flow (lower) relative to baseline for all cell conditions. 31

Figure 3—3 Retinal arteriolar diameter (upper), centerline blood velocity (middle) and blood flow (lower) attained at the low (left) and high (right) intensity laser settings for the no cell, 0.006% and 0.008% microsphere concentrations.....33

Figure 3—4 Densitometry profiles of a vessel measured by the CLBF (left) and schematic representation (right). Upper: baseline (no cell condition). Lower: 0.006% microsphere concentration. DW is the half-height width. 34

Figure 4—1 Bidirectional laser Doppler Velocimetry. A red diode laser (675nm, 80μm x 50 μm oval) is used to acquire bi-directional LDV measurements. The frequency shift of the light scattered by the moving blood cells at the illuminated site is simultaneously focused by two distinct photodetectors separated from each other by a fixed, known angle[41]. The maximum frequency shift detected by each photo-detector is subtracted to allow the absolute quantification of centerline blood velocity, irrespective of the angle between the moving particle and reflected beam[49;118]. The resulting Doppler signal is analyzed using a previously described algorithm[49]; the frequency shift is determined as the frequency at which there is an abrupt reduction in the amplitude of the fluctuations in the Doppler-shift power spectrum. This determination does not depend on any presumed shape of the average power spectral density curve. 40

Figure 4—2 Retinal vessel diameter is determined by projecting a rectangular (1500 μm x 150 μm) green (543 nm) HeNe diode laser perpendicular to the vessel segment measurement site. Densitometry analysis of the cross-sectional vessel image on the CLBF array sensor is used to calculate vessel diameter. The minimum point (Min_1) in the central portion of the image is designated as the nominal vessel center with D_1 being its signal level from the background level. When mirror reflection occurs from the vessel wall, the second minimum point is observed in the neighborhood of Min_1 with signal level D_2. The maximum points on either side are detected as the vessel edges with D_3 and D_4 signal levels. The half height points (X_1 and X_2) are points on the image whose signal levels are $(D_1+D_3)/2$ and $(D_2+D_4)/2$, respectively. The width between X_1 and X_2 is taken to represent the uncorrected vessel diameter and is converted into micron units after correction for axial and refractive magnification effects[45;119]. (Image courtesy of Canon Inc, Japan) 41

Figure 4—3 Boxplot (left) and Scatterplot (right) of each individual showing the retinal arteriolar diameter (upper), centerline blood velocity (middle), and blood flow (lower) measured pre- (i.e. cataract) and post-operatively (i.e. IOL). (IOL; intra-ocular lens). 46

List of Tables

Table 3—1. Group mean (± standard deviation) retinal arteriolar diameter, centerline blood velocity and flow as a function of artificial light scatter condition. 30
Table 3—2. Group mean (± standard deviation) retinal arteriolar diameter, centerline blood velocity and flow as a function of artificial light scatter condition and laser intensity.....32
Table 4—1 Group mean ± standard deviation (Median) retinal arteriolar diameter, centerline blood velocity and flow pre- and post-operatively (i.e. cataract and IOL, respectively) (IOL; intra-ocular lens). 45
Table 4—2 LOCS III system used to document the severity of cataract. Nuclear opalescence (NO), nuclear color (NC), cortical opacity (CO), post subcapsular (PS).....45
Table 4—3 Assessment of intra-ocular light scatter: Change in logMAR visual acuity between the high and low illumination settings of the Brightness Acuity Tester (BAT) using 10% and 96% contrast ETDRS charts.....45

1 Introduction

1.1 Ocular Circulation

Two separate vascular systems are involved in the ocular blood circulation; Retinal and uveal (ciliary) blood vessels. The uveal blood vessels include the vascular beds of the iris, the ciliary body, and the choroid[1].

Arising from the ophthalmic artery within the orbit, the central retinal artery (CRA) supplies approximately the inner 2/3 of the retina. The CRA pierces the optic nerve approximately 10-15 mm behind the globe, running parallel with the central retinal vein within the optic nerve[2]. It passes through the lamina cribrosa entering the optic disc just nasal to center and branches superiorly and inferiorly. These branches divide into nasal and temporal branches, and continue to bifurcate within the retinal nerve fiber layer below the transparent internal limiting membrane to supply the quadrants of the retina[3]. The tight junctions between the endothelial cells (zonula occludens) constitute the inner blood retinal barrier (BRB), preventing leakage of blood constituents into the retinal tissue for optimal retinal functioning.

The outer 1/3 of the retina, including the photoreceptors, is avascular and nourished from the highly vascularized choroidal circulation, derived from the ophthalmic artery via branches of the long posterior ciliary, short posterior ciliary, and anterior ciliary arteries. Specifically, the short posterior ciliary arteries supply the posterior choroid, while the long posterior ciliary arteries and anterior ciliary arteries supply the anterior choroid and the circle of the iris[4]. The anatomical border between the retina and the choroid is Bruch's membrane[5]. Adjacent to Bruch's membrane, the retinal pigment epithelium (RPE), acts as the blood-retina barrier and selectively transports nutrients and waste between the choriocapillaris and the neural retina[6]. The fovea centralis is completely avascular in terms of the inner retinal blood supply and totally relies upon the underlying choroid for metabolic supply and waste removal[2].

The veins of the orbit are tortuous and freely anastomose with one another and they have no valves or sphincters. The orbit is drained by the superior and inferior ophthalmic veins, which in turn drain directly into the cavernous sinus. The central retinal vein usually drains directly into the cavernous sinus or into the superior ophthalmic vein[4].

1.2 Retinal Blood Flow

Blood flow through a vessel is dependent on perfusion pressure and resistance to flow. Perfusion pressure is the difference between local arterial (Pa) and venous pressures. In the eye, venous pressure is assumed to be equal to intraocular pressure (IOP). Blood flow in the retinal vessels is consistent with Poiseuille's law of laminar flow[7-11].

1.2.1 Poiseuille's Law

Poiseuille's law states that in the case of smooth flow (laminar flow), the volume flow rate is given by the pressure difference divided by the viscous resistance. The resistance to blood flow is inversely proportional to the fourth power of the radius of the vessel and directly proportional to blood viscosity and the length of the vessel[7;11;12]. Poiseuille's law is found to be in reasonable agreement with experiments on uniform liquids (called Newtonian fluids) in cases where there is no appreciable turbulence[12].

$$F = \frac{\pi}{128} \times \frac{\Delta P}{\Delta L} \times \frac{1}{\eta} \times D^4$$

Where $\Delta P / \Delta L$ is the pressure drop per unit length of blood vessel, η is the blood viscosity, and D is the blood column diameter.

1.2.2 Autoregulation of Blood Flow

The goal of autoregulation in a tissue is to maintain relatively constant blood flow, capillary pressure, and nutrient supply, despite changes in perfusion pressure (mean arterial BP in vessels – IOP). Autoregulation of blood flow is achieved by alteration in resistance to blood flow and that in turn is affected by change in the diameter of the blood vessels. It is generally thought that the terminal arterioles regulate the resistance to flow, i.e. they dilate to increase the blood flow when the perfusion pressure falls and constrict to reduce the blood flow in arterial hypertension. Since there is a limit to how far the terminal arterioles can constrict or dilate, the autoregulation operates only within a certain critical range of perfusion pressure, and breaks down when the perfusion pressure goes below or above this critical range[11].

It is well known that retinal blood flow has an efficient autoregulation[11]. The choroid on the other hand is richly supplied by the autonomic nerves which are mainly responsible for vascular resistance. Recent studies have shown a modest autoregulation in the subfoveal choroid[2;13-15].

According to the metabolic hypothesis, local arteriolar smooth muscle tone is also regulated by the local concentration of metabolic products, pO_2 and pCO_2[16-18]. Conversely, the myogenic hypothesis states that rise of perfusion pressure causes vasoconstriction because stretching of the vessel wall is counteracted by vasoconstriction in the arterioles[19]. Endothelial derived vasoactive agents (Prostanoids, NO, endothelins, angiotensins, thromboxane A_2, etc.) are thought to be most probably responsible for initiating both the metabolic and myogenic contraction. Based on the neurogenic hypothesis, autoregulation is carried out by neural input in the vessels. This hypothesis is more relevant to the choroidal autoregulation as retinal blood vessels lack an autonomous innervation.

1.2.3 Blood Flow and Ocular Diseases

A mounting body of evidence suggests that vascular pathologies play an important role in the etiology and progression of number of ophthalmic diseases, including glaucoma, age-related macular degeneration, and diabetic retinopathy[2;20;21]. Our laboratory has shown reduced retinal vascular reactivity in diabetic patients[22-25]. Studies in glaucoma patients have shown reduced blood flow to the retinal ganglion cells and optic nerve, possibly contributing to the damage seen in glaucomatous optic neuropathy[21;26;27]. Changes in macular retinal capillary blood flow are also documented in age-related maculopathy[28]. In the future, the assessment of ocular hemodynamics may play a role in the early detection of some of the ocular diseases and possibly provide new insight of retinal disease that may offer new treatment options. Other possible uses are monitoring disease progression and evaluating the effectiveness of surgical and drug treatments.

1.3 Ocular Hemodynamic Assessment Techniques

The eye is the only location in the human body that allows for a direct, noninvasive observation of vascular blood flow. In this respect, the eye provides us with a unique opportunity to study ocular blood flow and investigate its characteristics in normal subjects and in patients with ocular diseases[2;21].

1.3.1 Pulsatility Measurement Devices

The pulsatile ocular blood flow device is a pneumotonometer that measures IOP in real time. The underlying concept is that IOP increases as the blood volume in the eye increases with the systolic pulse and decreases as the eye blood volume decreases during diastole. These fluctuations are then recorded as a function of time which is then transformed into volume fluctuations over time. Calculation of pulsatile ocular blood flow from the change in IOP is based upon a model eye assuming a standard ocular rigidity[29-31]. One of the weaknesses of this particular technique is that a universal relationship is used to convert IOP pulse wave into an ocular blood volume wave and the considerable individual variation in this relationship is ignored[2]. Some of the advantages are the affordable price of this device and that it is easy to operate.

Interferometry[32] is another technique used to directly measure the pulsation of the fundus relative to the cornea[2]. A single laser beam passes through the center of the eye and partially reflects from both cornea and retina. These two reflections form a stationary interference pattern which is a function of the distance between the two reflective sources[2;21]. The advantage of the interferometry is that it uses absolute units in micrometers to measure fundus movement. Excellent reproducibility is another major advantage of this technique. However, all pulsatility based measurement devices measure the secondary effects of blood flow upon some aspect of the eye and not the blood flow itself.

1.3.2 Angiography

Fluorescein dye was first used to assess retinal blood flow quantitatively by Hickam and Frayser[33]. Measurement of ocular hemodynamics by angiography is based on a dye dilution technique, where a known amount of a dye (or indicator) is injected into a vein and its arteriovenous passage time is observed at different points[21;34]. The concentration of the dye within the blood at an observation point is graphed against time and is called dye dilution curve. This technique is based on the concept that: Dye Flow Rate = Blood Flow rate x ($[I^p]$-$[I^d]$), where $[I^p]$-$[I^d]$ is the difference between the concentration of the indicator or dye proximal and distal to the area of the measurement[34].

Over the past decade, scanning laser ophthalmoscopes with confocal optics have improved the quality of images and allow high temporal resolution imaging. Two devices are currently commercially available, the Heidelberg Retina Angiograph (HRA) system and the Rodenstock scanning laser ophthalmoscope (SLO).

Fluorescence angiography is invasive and is not a good technique to assess patients in the later stages of retinopathy as vessels might leak the fluorescein and the visualisation of the dye becomes more difficult[35]. Although scanning laser ophthalmoscopy has dramatically improved angiography, the instrument is very expensive and a skilled and experienced user is needed to obtain high quality angiograms. Media opacities also limit the quality of the images[36].

1.3.3 Retinal vessel analyzer

This instrument assesses change in diameter (relative units) but is not capable of measuring blood velocity or flow. An image of the fundus is displayed on a monitor for real time inspection. A region of interest is defined by the examiner and the diameter of the vessel (arteriole, venule, or both) inside this region is determined using an algorithm that detects the vessel edges at a maximum frequency of 50Hz[37]. Change in vessel diameter is expressed as a function of time or relative position along a vessel[38].

1.3.4 Color Doppler Imaging

Color Doppler imaging (CDI) was first technique used to image blood flow in the heart and large vessels such as carotid artery[39]. At the present time it is also used in ophthalmology mostly to measure blood velocity in the ophthalmic artery, central retinal artery, and posterior ciliary arteries which are all located immediately behind the globe and supply the eye[40]. Doppler shift is the change in frequency of the sound wave when it reflects off a moving object (in this case red blood cells). This shift is directly proportional to the magnitude of the velocity. The Doppler shift is calculated using the following formula:

$$\Delta F = \frac{2 f_0 V_{blood}}{V_{sound}} Cos\theta$$

where ΔF is the Doppler shift, f_0 is the frequency of the ultrasound beam, V_{blood} is the velocity of the red blood cells creating the Doppler shift, V_{sound} is the velocity of the ultrasound through the body, and θ is the angle between the incident beam and the direction of movement of the red blood cells[21].

The strength of the CDI is its ability to image patients with poor ocular media as it uses sound waves rather than laser. A clear view of the fundus is not required; therefore pupil dilation is not necessary. One of the limitations of this technique is that it requires an experienced technician to get reproducible data; variation of the angle Θ will result in large differences of blood velocity. Also if the probe is pushed strongly against the eyeball it can change the IOP and in turn the velocities being measured. This device cannot quantify flow as it does not measure vessel diameter and it is a very expensive technology.

1.3.5 Laser Based Instruments

Laser has been used as a surgical treatment tool since 1960[41]. Two properties of the laser make it suitable to be used in the clinical settings for surgical purposes; its high intensity and low beam divergence. Recently, another two properties of the laser are used to develop diagnostic tools, that is the monochromaticity and coherence of the emitted light.

1.3.5.1 Laser Doppler Flowmetry

The laser Doppler flowmeter (LDF) is a laser Doppler device which examines the volumetric flow in the capillary beds of the retinal tissue and not in large vessels. Petrig and colleagues[42] showed that flow measurements could not distinguish between choroidal and retinal sources of Doppler shifts. Therefore, LDF is only used to measure subfoveal choroidal blood flow and optic nerve head microcirculation[2;41].

The laser is focused onto a 50 μm diameter circular area of the fundus and then the scattered light is collected by a photodetecter from a larger circular area (150 μm) of the fundus surrounding the laser spot[2;41]. By collecting the scattered light from a larger area surrounding the incident beam, laser light can scatter deeply into the tissue being measured. The interference pattern between the Doppler shifted and non Doppler shifted frequencies are then analyzed by

LDF to derive localized volumetric blood flow measurements. LDF is limited to the assessment of certain sites as described above and blood flow values are in arbitrary units which have poor reproducibility[2;43].

The Heidelberg Retina Flowmeter (HRF, Heidelberg Engineering, Germany) is a confocal scanning version of the LDF. Using this technique, the HRF laser repeatedly sweeps the fundus. HRF measurements tend to be concentrated on surface vasculature because it only analyzes the scattered light from the illumination point which prevents the laser from penetrating deep in the tissue[2]. Work from our laboratory has shown that artificially induced light scatter erroneously elevates HRF values[44].

1.3.5.2 Laser Doppler Velocimetry

Bidirectional laser Doppler velocimetry (LDV) is a technique used to measure the maximum red blood cell velocity in the large retinal vessels[21;45]. In the bidirectional technique, one incident beam is used to illuminate a site along a retinal vessel. The light scattered by the blood cells at the illuminated site is detected simultaneously by two distinct detectors separated from one another by a fixed known angle[41] (Figure 1—1). Maximum velocity of the red blood cells are then determined according to the following two formulas:

$$\frac{\Delta f_{maxA}}{\Delta f_{maxB}} = \frac{\mathrm{Cos}\,(\theta+\alpha)}{\mathrm{Cos}\,\alpha} \qquad \Delta f_{\max A} - \Delta f_{\max B} = \frac{2\,V_{max}\,\mathrm{Cos}\alpha}{\lambda}$$

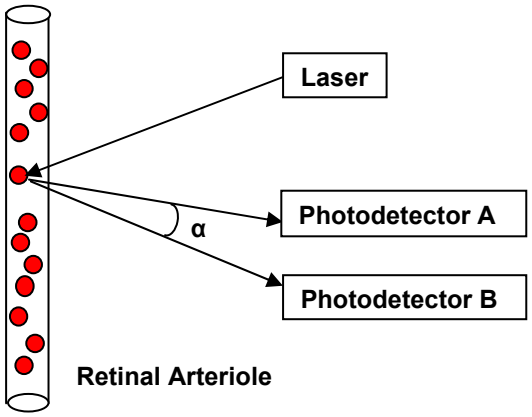

Figure 1—1. Bidirectional laser Doppler Velocimetry.

V_{max} is then used to derive V_{mean}. In a turbulent flow system, $V_{min}=V_{max}$, however, in most situations a laminar flow is assumed such that, $V_{mean}= ½ V_{max}$. Other prominent researchers in the field utilized a factor of 1.6 to derive V_{mean} from V_{max} (i.e. $V_{mean} = V_{max}/1.6$)[7;45;46], however, $V_{mean}= ½ V_{max}$. is now generally accepted to described the relationship of these two factors, at least in relatively straight vessel segments of minimum diameter 50um and distant from bifurcations. Average volumetric flow can also be computed if the corresponding vessel diameter (D) is measured[45]:

Blood Flow = $½ (\pi.D^2/4) V_{mean}.60$

This calculation assumes that the vessel has a circular cross section which is not always the case but the errors introduced by this assumption are very small[47].

Early instruments developed by Riva et al.[48] and Feke et al.[49] comprised a fundus camera or slit lamp, respectively, to which a laser and photodetectors were attached for the assessment of retinal hemodynamics. These early instruments, based on the concept of the bidirectional LDV, were difficult to use for anyone other than their developers. One difficulty was getting centerline blood velocity measurements despite the subjects' eye movements which would put the incident beam off the vessel center or off the vessel completely[41].

1.3.5.3 Canon Laser Blood Flowmeter

The Canon Laser Blood Flowmeter (CLBF) utilizes new technology to overcome the problems of the bidirectional LDV mentioned above. In order to lock the laser beam on the center of the vessel despite minor eye movements, Feke *et al.*[50] developed an eye tracking mechanism. Eye tracking is achieved by projecting a stripe shape from a green HeNe laser (544 nm, 1500x150 μm rectangular) through a beam steering galvanometer system onto the retinal vessel of interest. The green laser is manually manipulated by the operator in order to be oriented perpendicular to the vessel segment being measured. The image of the vessel and superimposed stripe is incident on an array sensor which detects any lateral motion of the vessel, and controls the steering system to stabilize the center of the green tracking stripe on the center of the vessel. The beam from a red diode laser (675nm, 80x50 μm oval) is the laser Doppler measuring source. The

beam is centered on the green stripe so that it also is stabilized on the target vessel[41]. The red laser is used to measure velocity every 0.02 seconds across a 2 second measurement window resulting in a velocity-time trace. The retinal vessel diameter is also measured using a densitometry technique from the signal produced by the image of the vessel on the array sensor. Diameter readings are acquired every 0.04 seconds during the first and final 60 milliseconds of the 2 second velocity measurement window. Two sequential measurements (path 1 and path 2) both of blood velocity and of vessel diameter are taken to ensure consistency of each parameter and are then averaged to give one reading.

The axial length of the eye needs to be input in the instrument and ocular refractive error is automatically measured by the instrument itself. Magnification effects associated with refractive and axial components of ametropia are corrected to provide absolute measurements of diameter (μm), velocity (mm/sec) and flow (μL/min).

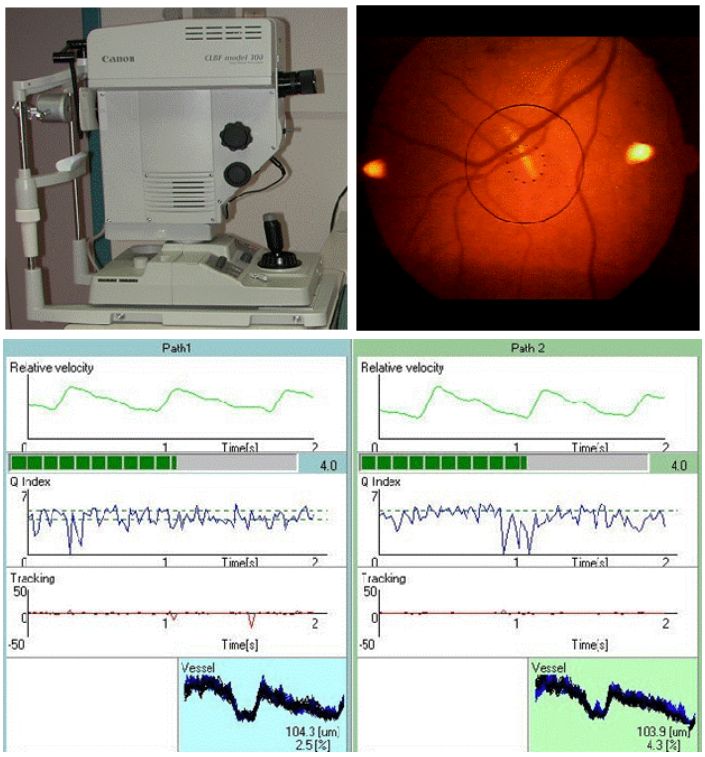

Figure 1—2. Top Left: CLBF model 100, top right: operator's view showing the green laser locked on a branch of retinal vessel, bottom half: measurement window showing blood velocity curves and densitometry profile of the vessel diameter.

One of the many advantages of the CLBF is the simultaneous measurement of the blood velocity and vessel diameter in only 2 seconds. Furthermore, CLBF is currently the only instrument that provides us with absolute measurements of the retinal blood flow rate in µl/min[2;21;41;45]. One limitation is the difficulty of obtaining results from patients with poor optics.

A recent study showed a strong correlation between both volumetric blood flow and velocities found by the CLBF, and central retinal artery blood velocities found by Color Doppler Imaging[51]. The CLBF has been extensively evaluated in clinically normal subjects and those with various types of retinal diseases[10;52;53]. Multiple studies have shown good repeatability and reproducibility of the CLBF measurements with low variability[10;54;55]. Therefore, the CLBF can be used for reliable comparison of blood flow characteristics at different retinal vascular sites in the same eye, at comparable sites in both eyes, and for comparison between patients and healthy control subjects[53].

1.4 Cataract

Except for the most developed countries where surgical correction is widely available, cataract is the leading cause of blindness worldwide[56]. The prevalence and incidence of cataract increases with increase in age [57].

1.4.1 Optical Changes

Light entering the eye can be scattered by optical imperfections. This scattering is subdivided into light scattered towards the retina (forward scatter) and light scattered backwards towards the source (backscatter). Back scattered light is usually not equal to forward light scatter and one cannot be directly deduced from the other[58]. The healthy human lens light scatter is less than 5%, and the contribution from the lens is approximately 50% of the total scattering in the eye[59]. Different parts of the lens have different scattering characteristics[60]. Both loss of light energy due to absorption and the scattering of light reduce the contrast of the retinal image. Forward light scatter is responsible for the reduction of the retinal contrast and therefore the assessment of forward light scatter is a more valid reflection of visual performance in glare conditions than backward scatter.

According to the scatter theory and studies on excised lenses, light scattering in the lens is wavelength dependent[59;60]; however, this is contradictory to many of the psychophysical measurements[59]. Light scatter in donor lenses increases monotonically from 700nm towards 400nm[59;60]; therefore, there is a greater degree of scatter for shorter wavelength light. This wavelength dependency varies by age and is greater in older subjects[60].

Various studies have documented increase in the ocular light scatter as a function of age using different methods[58;61;62]. Lens light scatter and transmission indices both change gradually until middle age and then a rapid change follows later in life with increase in the variability between subjects. Except for the lens, other refractive components of the eye (e.g. cornea) show little or no age-dependent change in the transmittance of light[63].

Since the lens does not shed any of its cells, all the cellular components from embryonic development onward are retained. The older cells of the lens, which are displaced toward the

center, experience progressive compaction, reduced metabolic activity and ageing. The lens becomes increasingly coloured (yellow) with age, more so in people with diabetes due to increased glycation, and the intrinsic fluorescence also increases, thereby increasing the absorbance of blue light[64-66].

In summary, throughout life lens transparency decreases causing increase in the intraocular light scatter and decrease in the spectral transmittance. These changes are more severe in the cataractous lenses causing more dramatic visual problems than mere ageing. The yellowing of the lens impacts color perception. Changes in the refractive error are also common in cataract, in particular increasing myopia and astigmatism. These refractive changes can be corrected with spectacles. However, changes in the structure of the lens may result in pockets of lens material with different refractive indices, which cannot be corrected adequately with spectacles[67;68].

1.4.2 Common Types of Cataract

There are three main morphological types of cataract: nuclear, cortical, and posterior subcapsular. Nuclear cataracts result from excessive nuclear sclerosis and yellowing, with consequent formation of a central lenticular opacity. In some instances, the nucleus can become very opaque and brown, termed a brunescent nuclear cataract.

Changes in the ionic composition of the lens cortex and the eventual change in hydration of the lens fibers produce a cortical cataract. Cortical cataracts are wedge-shaped opacities in the lens periphery which progress toward the center. Vision is not affected until these spokes intrude the pupil area[67;68].

Posterior subcapsular cataracts form when abnormal epithelial cells and extracellular granular and fibrillary material aggregate in the posterior subcapsular cortex and make plaque like opacities[67-69]. Even mild posterior subcapsular cataracts can drastically impact vision as these opacities are located in the center of the pupil area.

Pure forms of cataract, with only one type of opacity present, are usually found in the early stages of the disease, but as it becomes more severe, several types of opacity often co-exist in the same lens[70].

1.4.3 Etiology of Cataract

1.4.3.1 Congenital Cataract

Among 100,000 births, 30 infants are born with congenital cataract either in isolation or as part of a more complex syndrome[71]. Approximately 30% of these cases are hereditary with the majority involving autosomal dominant genes, although autosomal recessive and X-linked forms are also known[72]. Responsible genes may also play a role in some cases of age-related cataract[73].

1.4.3.2 Genetic Factors

In two separate studies, extracted human lens epithelial cells of cataract patients revealed down regulation of 262 to 412 genes and up regulation of 7 to 919 genes compared with cells from normal lenses[74;75]. All these data suggest a multi-factorial nature of the age-related cataract and the complexity of the genetic factors involved[72].

1.4.3.3 Age

Ageing causes changes in the structural, optical, and molecular characteristics of the lens which in turn increases the intraocular light scatter, leading to slow but steady development of cataract throughout life. However, some of these changes are accelerated in the cataractous lenses compared with age matched normal lenses. For example, formation of high-molecular weight protein aggregates accompanies ageing, but the process is greatly accelerated in cataract development[70].

1.4.3.4 Environmental Factors

The UV range of wavelengths in sunlight are the most significant environmental factor contributing to the development of cataract in humans[76]. Although most studies have emphasized the risks of UVB in cataract development, both UVA (320-400nm) and UVB (290-320nm) are thought to play significant roles in human cataract[77]. Exposing rats to UVA plus UVB has shown to cause much greater loss of lens transparency than either one alone[78].

1.4.3.5 Oxidative Stress

Reduced levels of glutathione is evident in most forms of cataract which might indicate a loss of the ability of the lens to withstand oxidative stress or that the protective mechanisms have been overcome[1;70]. One of the damages of the oxidation to the lens is modification of its protein structures. There is a little protein oxidation observed in the young lenses and only relatively minor oxidative changes are seen in the proteins of older clear lenses. In cataractous lenses, however, extensive oxidative modification of proteins is evident. Lenses incubated in the presence of hydrogen peroxide certainly demonstrate electrolyte imbalance, increased permeability, and reduced transport ability by oxidation[1]. Smoking is strongly associated with nuclear cataract using a variety of study designs[79-81]. Smokers seem to have lower ability to cope with oxidative stress in general, and several constituents of cigarette smoke are capable of causing chemical modification of lens proteins[70].

1.4.3.6 Metabolic Disorders

Electrolyte balance and consequently normal hydration of lens fiber cells are extremely important for maintaining the transparency of the lens. Therefore, metabolic disorders such as diabetes mellitus, and renal failure could potentially lead to lens opacification. For instance, risk of developing cataract is 12 times higher in patients with renal failure which may be due to accumulation of urea leading to carbamylation of lens proteins[82]. Cataract can develop rapidly in uncontrolled diabetes mellitus[1;83;84]. Hypoglycemia in newborn infants is known to cause cataract due to inability of the lens to produce sufficient metabolic energy[1].

1.4.3.7 Trauma

The lens becomes white soon after the entry of a foreign body, since interruption of the lens capsule allows aqueous and sometimes vitreous to penetrate into the lens structure[1]. Electric shock is another rare cause[82].

1.4.3.8 Drug-Induced Changes

Corticosteroids administered over a long period of time, either systemically or topically, can cause lens opacities. Other drugs associated with cataract include phenothiazines, amiodarone, and strong miotic drops such as phospholine iodide, used in the treatment of glaucoma[1].

1.4.4 Prevention & Management

1.4.4.1 Antioxidants and Nutritional Supplements

Use of antioxidants such as vitamins A, C and E is suggested as a preventive method to minimize oxidative damage to the lens[85]. Other pharmaceutical interventions such as Beta-Carotin and alpha-tocopherol are also tested as 'anticataract' drugs[86]. However, no drug or nutritional supplement to date has shown any significant result to reduce cataract or stop its progression in human. Some 'anticataracts' have lead to side effects and yet others have not proven efficient and successful. Therefore, use of any antioxidants or nutritional supplements has very little impact, if any, on cataract development and progression[87].

1.4.4.2 Surgical Management

Surgical removal of the cataractous lens and replacing it with an intraocular lens has been the single most effective treatment of cataract and it is now more efficient than ever before. With the use of phacoemulsification procedure, cataractous lens can be extracted through a 3mm limbal incision under local anesthesia. Intraocular lens is folded and put in place through the same opening. The smaller incision means fewer complications including collapse of the contents of the eye during surgery and suture-induced astigmatism[88]. Cataract surgery is very successful as documented in numerous studies showing improved visual functions. According to one study by Rubin et al. [89], following surgery, most patients' scores on visual acuity, contrast sensitivity and glare disability returned to normal. They also claim that patients were equally likely to regain normal visual function after surgery regardless of their preoperative vision. Patients also experience better color perception after cataract surgery and better quality of life. The most common post operative complication of cataract surgery is posterior capsule opacification (PCO), which occurs in about 25% of the cases, usually 5 years after the surgery. It is most commonly treated by laser capsulotomy (Nd-YAG; wavelength 1064nm) in the clinic while patient is sitting upright and fixating on a target. The goal of laser capsulotomy is to open a hole in the posterior capsule, allowing improved clarity of the visual axis and therefore better vision[88]. Other complications which are routine to all surgeries are very rare and occur in less than 2% of the cases[88].

1.4.5 Grading Cataract

It is very important to be able to classify and grade lens opacities for clinical use and also for epidemiological studies trying to find underlying causes of cataract. It is not only important to consider the location of the lens opacity but also to document its intensity and size. Various classification systems exist; some assess the morphology of the lens using the slit-lamp (LOCS, OCCCGS) and some assess the change in visual function.

1.4.5.1 LOCS III

The Lens Opacities Classification System III (LOCS III) photographic set consists of six slit-lamp images for grading nuclear color and nuclear opalescence, five retro illumination images for grading cortical cataract, and five retro illumination images for grading posterior subcapsular cataract. Cataract severity is graded on a decimal scale, and the standards have regularly spaced intervals on a decimal scale[90]. With 0.1-unit intervals, nuclear color and nuclear opalescence scores summarize the nuclear color or opacity of the lens in one numeric dimension between 0.1 (colorless or clear) to 6.9 (brunescent or very opaque). In cases of cortical and posterior subcapsular cataract, the scale ranges from 0.1 to 5.9 [91]. LOCS III has great reproducibility with 95% tolerance limits of 0.4 to 1.0[90].

1.4.5.2 OCCCGS

The Oxford Clinical Cataract Classification and Grading System (OCCCGS) is another composite slit-lamp based system that employs standard diagrams and Munsell colour samples to grade specified features in different anatomical zones in the lens[67;68;92]. Sparrow and colleagues[93] developed a decimal version of the Oxford system with finer scale intervals, which substantially improved its reliability due to higher levels of repeatability and scale sensitivity.

1.4.5.3 Visual Acuity and Contrast Sensitivity

LogMAR visual acuity (VA) and contrast sensitivity (CS) scores are associated with the severity of some types of cataract[94;95]. Nuclear cataract impacts VA and CS the most and cortical opacities the least[94].

VA is widely used in clinical settings for visual assessment of patients with cataract. However, it is not an adequate assessment of vision in these patients as some have relatively good VA but

suffer from poor dynamic visual performance. CS is suggested by some researchers to be an important test along with VA for assessing cataract patients[89].

As seen in the following graph, both patients with refractive error and increased light scatter have approximately the same high contrast VA but the later one is more likely to have poorer vision in everyday life. Pelli-Robson CS or low contrast VA tests would be better to assess visual function in this case. The Pelli-Robson chart consists of rows of letters of the same size but decreasing contrast which gives an indication of CS just below the peak of the CSF curve (0.5-2 c/d)[67;68].

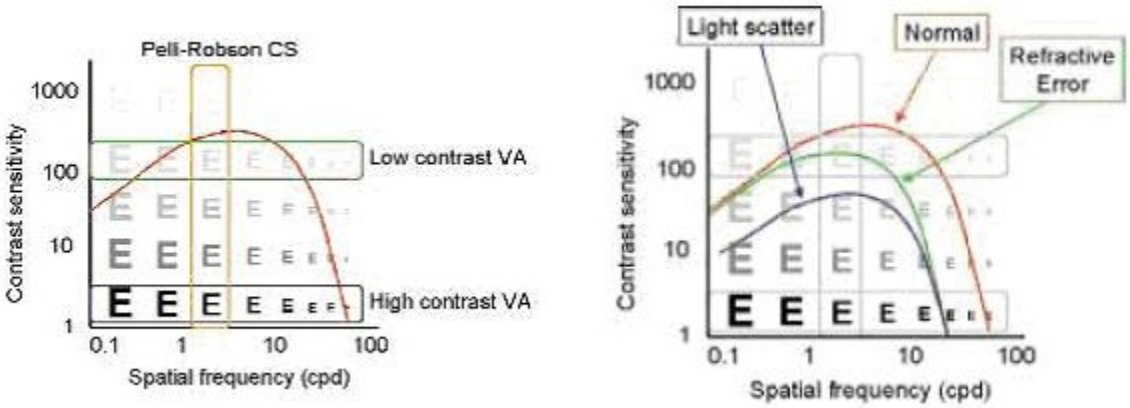

Figure 1—3. (a) contrast sensitivity function (CSF), (b) comparison of CSF for normal, refractive error and increased light scatter[68]. (Image reproduced by permission of OT, the magazine of the Association of Optometrists, www.optometry.co.uk)

Small letter CS test (high spatial frequency) is thought to be more sensitive to early cataractous change than both large letter CS (low spatial frequency) and VA[96]. Furthermore, large letter CS is more relevant in the assessment of patients in the later stages of cataract development as they hardly see any of the small letters[89;96;97]. High correlation between VA and high spatial frequency CS ($r^2 = 0.70$) makes it less likely to be used in clinical settings in addition to VA[96]. Other studies have also shown that CS provides little information beyond VA in visual assessment of patients with cataract[94;98;99].

1.4.5.4 Brightness Acuity Tester

Forward light scatter is one of the characteristics of cataract that causes reduced contrast of image on the retina. Forward light scatter becomes more problematic when the light level differs largely in different parts of the visual field (e.g. when the sun is low in the sky or when viewing

oncoming car headlights at night). This phenomenon is known as disability glare[67;68;100]. The Brightness Acuity Tester (BAT) provides measurements of functional visual acuity under three different lighting levels which mimic everyday lighting conditions. It consists of an internally illuminated hemispherical bowl with a hole in the middle. It is a handheld instrument that patient holds and looks at the chart through the opening. This provides a bright uniform glare source that can be used in conjunction with VA and CS tests.

1.4.5.5 Potential Acuity Meter

The Potential Acuity Meter (PAM) is a test for assessing retinal function in patients with cataract. The PAM uses a single channel Maxwellian view projection system to image a letter chart onto the patient's retina. The Maxwellian view arrangement ensures that the light source is imaged in the plane of the patient's entrance pupil thereby ensuring that a very narrow beam of light passes through the lens[67;68]. The examiner minimizes the effects of the cataract by selecting a relatively clear portion of the lens. Several factors such as visual acuity of 20/200 or worse, the type and severity of the cataract, and coexisting retinal disorders may affect the accuracy of the PAM[101].

1.4.5.6 Straylight Meter

Van den Berg developed an idea originally proposed by Le Grand (1937) to directly measure the light scatter function of the human eye[2;67;68]. The Straylight Meter is a device that measures intraocular stray light by using the psychophysical direct compensation approach[100;102].

Vision in elderly can be affected by increase in lens opacity and also by neuronal degradation of retina (i.e. photoreceptor loss, and/or axonal loss in the optic nerve). Visual acuity and contrast sensitivity tests are influenced by loss of neuronal function as well as lens opacity. Measuring Forward light scatter has the advantage of being relatively free from neuronal interactions[103]. Several studies have shown that forward light scatter is a better, more sensitive predictor of functional vision loss in patients with lens opacities than visual acuity and contrast sensitivity[89;103;104].

1.4.5.7 Scheimpflug camera

There are several commercially available cameras that use Scheimpflug principle and are capable to image the entire anterior segment of the eye in vivo. This will allow researchers and clinicians to document 3-D arrangements of the lens opacities and evaluate intraocular light scatter conditions. Image analysis is based on peak height and distance evaluation of 2 layers in the cornea and 10 layers in the lens[105]. The Scheimpflug principle requires that the plane containing the slit beam and the image plane intersect at one point, with the corresponding angles equal[106].

1.5 Simulated Light Scatter Model

An artificial light scatter model has been used in various studies to induce light scatter. The impact of simulated light scatter has been studied on the outcome of clinical automated perimetry[107-109], digital retinal imaging[110], HRF[44], and HRT[111].

Suspension of varying concentrations of 0.5μm polystyrene microspheres could be used to create light scatter that increases as more concentrated suspensions are used. These solutions can be injected in a cell apparatus made up of two plano lenses enclosed in a plastic collar, which can be placed close to the subjects' eyes to create light scatter. A bead diameter of 0.5μm was selected as the diameter of the protein aggregates in human cataractous lenses is shown to be between 300 and 500 nm[112].

1.6 Summary

Ocular circulation, blood flow and various hemodynamic assessment techniques were reviewed here. One of the laser based instruments reviewed is the CLBF, used extensively in our lab and elsewhere to investigate the physiology of retinal hemodynamics[17;113;114] and the pathophysiology of hemodynamic disturbance in diseased states such as diabetes[113;115;116].

Cataract was also addressed in this introduction. There are many ways to grade cataract and quantify the amount of intraocular light scatter produced by cataract, which were discussed here. A simulated light scatter model has also been developed to study the impact of light scatter on different instruments which mimics the impact of cataract. The impact of light scatter due to

cataract on the outcome of retinal hemodynamic assessment techniques, such as that used in the CLBF, is unknown.

2 Rationale

The eye is regarded as a window to the human body providing us with a unique opportunity to use non-invasive methods and to directly visualize the retinal vasculature. The retinal circulation has been studied in normal and diseased states and hemodynamic disturbances have been documented in some ocular diseases. Assessment of retinal hemodynamics enables us to study the pathophysiology of the disease, and might in the future allow us to monitor its progression and response to various treatment modalities, and perhaps in the near future assist us in early detection of not only the ocular diseases but also other systemic illnesses with ocular manifestations.

The CLBF is a novel instrument used to assess retinal hemodynamics; it measures blood vessel diameter and velocity and calculates the blood flow, all in real units. There are other instruments using similar algorithms to measure vessel diameter and yet others that use different techniques to assess retinal blood flow. Some of these instruments including the CLBF are impacted by the intraocular light scatter as they rely on the clear media allowing light to pass to the retina and return to the detectors with minimal interference from the lenticular opacity. The impact of light scatter on the CLBF has never been studied despite its wide use in the elderly population where increase in the intraocular light scatter is always observed and concomitant cataract is almost inevitable.

The overall aim of this project was to investigate the impact of light scatter on the retinal hemodynamic measurements and to investigate ways to minimize this impact. In the first study, young healthy subjects were recruited and light scatter was induced using the artificial light scatter model developed by Hudson et al[110]. Induced light scatter was increased by using more concentrated solutions in the lens apparatus that was placed in front of the CLBF and serial measurements were acquired from the same vessel segment on a retinal arteriole. Our hypothesis was that the induced light scatter would impact the CLBF measurements. In the second study, we further studied this impact by imaging real patients undergoing cataract surgery. Several measurements of the same spot on a retinal arteriole were acquired using the CLBF, before and after the surgery. Our hypothesis was that measurements acquired before (i.e. opaque media) and

after the surgery (i.e. clear media) would follow the same trends we found with the artificial light scatter model.

The findings of this project would not be limited to the CLBF as there are many other instruments using similar algorithms. These instruments are widely used to investigate the disease processes in elderly population often over a period of time where not only the concomitant cataract can impact the results but also an increase in intraocular light scatter over the period of the study is inevitable, impacting the measured entities and introducing a bias in the results.

3 Impact of simulated light scatter on the CLBF

Impact of simulated light scatter on the quantitative, noninvasive assessment of retinal arteriolar hemodynamics.

Azizi B, Buehler H, Venkataraman ST, Hudson C.

Journal of Biomedical Optics. 2007; 12(3): 034021

	Concept / Design	Recruitment	Acquisition of data	Analysis	Write-up / publication
Azizi	X	X	X	X	X
Buehler	X				
Venkataraman	X				
Hudson	X			X	X

Table detailing role of each author in this publication (X denotes significant contribution)

3.1 Introduction

The potential of non-invasive retinal imaging techniques to investigate the physiological mechanisms regulating blood hemodynamics in the human retina have long been recognized. However, techniques are now available that permit the non-invasive quantification of volumetric retinal blood flow in absolute units by simultaneously measuring vessel diameter (μm) and centerline blood velocity (mm/sec) to derive flow in real units (μl/min)[10;53;55]. Blood flow assessments using the Canon Laser Blood Flowmeter (CLBF) are repeatable and reproducible with low variability[2;11;21].

Disturbance of retinal blood flow is a feature of many ocular diseases[1;117], including diabetic retinopathy[1;11;22;35;117], age-related maculopathy[28], and a subset of patients with glaucoma[21;27]. In the future, the assessment of retinal blood flow may play a diagnostic role in the early detection of some of these ocular diseases[22]. Retinal hemodynamic assessment techniques may also be used to monitor aspects of disease progression and to evaluate the retinal vascular response to surgical and drug treatments[21].

Lens opacity, or cataract, frequently occurs concomitantly with other eye diseases, including diabetic retinopathy, age-related maculopathy and glaucoma. The impact of lens opacity on the assessment of retinal blood flow is unknown, despite the fact that the technique has been used widely in elderly subjects. The clarity of fundus visualization using any fundus camera based imaging device is limited in the presence of lens opacity due to intraocular light scatter that results in reduced image contrast. Recent studies from our group have quantified the influence of artificial light scatter on various retinal imaging instruments[44;110;111]. The present study was designed to determine the impact of artificial light scatter on quantitative measurements of retinal arteriolar hemodynamics.

3.2 Methods

One eye from each of 10 healthy young subjects between the ages of 18 and 30 (mean age 23.6 years, SD 3.4) was randomly selected. All volunteers were informed about the details of the study and gave their consent to participate. The research followed the tenets of the Declaration of Helsinki and was approved by the Research Ethics Board of the University Health Network and also by the Office of Research Ethics of the University of Waterloo. All subjects were drug free with no systemic disease, no ocular abnormalities and no history of any ocular surgery. Subjects had no lens opacity, exhibited intra-ocular pressures less than 21 mmHg, a logMAR visual acuity of 0.0, or better, and a refractive error < ±6.00 DS and < ±2.50 DC.

Artificial Light Scatter Model

The details of the artificial light scatter model have been published elsewhere[44;110;111]. In brief, cells comprising a plastic collar and two plano lenses were filled with solutions of differing concentrations of polystyrene microspheres[110] (Polybead© Polysciences Inc., USA). The diameter of the microspheres was chosen to be similar to the mean diameter of aggregated lens proteins (500nm) that are thought to produce intraocular light scatter in the normal ageing lens. Microsphere concentrations of 0.002%, 0.004%, 0.006%, and 0.008% were made up from a 0.16% stock solution and a distilled water only cell was also utilized to act as a further control i.e. anticipated not be different from baseline. The microsphere concentrations were determined empirically prior to commencing the study by imaging subjects using the CLBF and determining the point at which the instrument could no longer reliably stabilize a given measurement site. Solutions were made-up and the cells were emptied, cleaned and refilled every week. Cells were also checked regularly with a spectrophotometer to ensure consistency of the optical transmission and absorption characteristics throughout the course of the study.

Quantitative Assessment of Retinal Arteriolar Blood Flow

Quantitative Assessment of retinal arteriolar blood flow were acquired using the Canon Laser Blood Flowmeter (CLBF), model 100. The CLBF utilizes bidirectional laser Doppler velocimetry (LDV) to quantify the centerline blood velocity in the large retinal vessels, densitometry to measure vessel diameter and an image stabilization system to minimize the impact of eye movement[21;45]. A red diode laser (675nm, 80μm x 50 μm oval) is used to acquire

bi-directional LDV measurements. The frequency shift of the light scattered by the moving blood cells at the illuminated site is simultaneously focused by two distinct photodetectors separated from each other by a fixed, known angle[41]. The maximum frequency shift detected by each photo-detector is subtracted to allow the absolute quantification of centerline blood velocity, irrespective of the angle between the moving particle and reflected beam[49;118]. The resulting Doppler signal is analyzed using a previously described algorithm[49]. The frequency shift is determined as the frequency at which there is an abrupt reduction in the amplitude of the fluctuations in the Doppler-shift power spectrum. This determination does not depend on any presumed shape of the average power spectral density curve. Velocity measurements are acquired automatically every 0.02secs throughout the 2secs measurement window, resulting in a velocity-time trace that depicts the systolic-diastolic variation of blood velocity.

Retinal vessel diameter is determined by projecting a rectangular (1500 μm x 150 μm) green (543 nm) HeNe diode laser perpendicular to the vessel segment measurement site. Densitometry analysis of the cross-sectional vessel image on the CLBF array sensor is used to calculate vessel diameter (Figure 3—1). The minimum point (Min_1) in the central portion of the image is designated as the nominal vessel center with D_1 being its signal level from the background level. When mirror reflection occurs from the vessel wall, the second minimum point is observed in the neighborhood of Min_1 with signal level D_2. The maximum points on either side are detected as the vessel edges with D_3 and D_4 signal levels. The half height points (X_1 and X_2) are points on the image whose signal levels are $(D_1+D_3)/2$ and $(D_2+D_4)/2$, respectively. The width between X_1 and X_2 is taken to represent the uncorrected vessel diameter and is converted into micron units after correction for axial and refractive magnification effects[45;119]. Diameter measurements are acquired every 4msecs during the first and last 60msecs of the 2 second velocity acquisition window.

An integral "eye tracking" mechanism stabilizes the laser system on the selected measurement site. Light from the red laser is projected into the center of the green rectangle[41]. The green laser is manually adjusted perpendicular to the vessel segment. The resulting cross-sectional image of the vessel is focused on the CLBF array sensor. The array sensor detects any lateral motion of the vessel and, via a negative feedback loop, controls the galvanometer steering system to

stabilize the green tracking laser on the selected measurement site. This system also permits identification, and post-acquisition rejection, of velocity measurements impacted by significant saccades.

Two sequential measurements (Path 1 and Path 2) both of blood velocity and of vessel diameter are taken to ensure consistency of each parameter and are then averaged to give one reading. V_{mean}, the time average of the centerline blood velocity, is used along with the diameter, D, to calculate retinal blood flow, F, assuming that the vessel has a circular cross section and that the flow characteristics obey Poiseuille's law. Retinal blood flow is derived using the formula: $F = ½ (\pi . D^2/4) (V_{mean} . 60)$, where flow is in µl/min, diameter is in µm and V_{mean} is in mm/sec. Magnification effects associated with refractive and axial components of ametropia are corrected to provide absolute measurements of diameter (µm), velocity (mm/sec) and flow (µL/min).

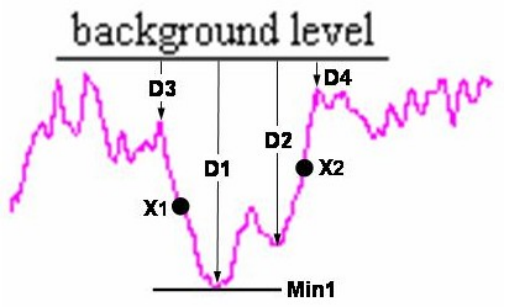

Figure 3—1 Densitometry signal of a cross-sectional image acquired from a retinal arteriole. Min_1; minimum point in the central portion of the image designated as the nominal vessel center. D_1; signal level of Min_1 from the background level. D_2; signal level of the second minimum point in the neighborhood of Min_1. D_3 and D_4; signal levels of the maximum points on either side designated as the vessel edges. X_1 and X_2; the half height points whose signal levels are $(D_1+D_3)/2$ and $(D_2+D_4)/2$, respectively. The width between X_1 and X_2 is taken to represent the uncorrected vessel diameter. (Image courtesy of Canon Inc, Japan)

Procedures

Each subject underwent screening that included the assessment of general and ocular health, best corrected logMAR visual acuity, anterior segment examination, assessment of crystalline lens

status (using the Lens Opacity Classification System, LOCS, III) and fundus examination. The randomly selected study eye was dilated using Mydriacyl 1% (Alcon Canada Inc. Mississauga, Canada). Retinal arteriolar hemodynamics were then measured in a superior temporal arteriole. The measurement site was selected in a relatively straight vessel segment, distant from any bifurcations and within 1 disc diameter of the optic nerve head. Initial measurements were acquired with no cell in place as a baseline to optimize and set the instrument focus and positioning. Retinal hemodynamics measurements were then acquired at the same measurement site (using the fixation target memory feature of the CLBF) while placing cells of various microsphere concentrations in front of the subjects' eye in random order. The randomization was implemented in order to negate the impact of any potential drift of CLBF values or systematic change of hemodynamic parameters. The cells were mounted to the objective of the CLBF using a custom made adaptor that incorporated a 20° tilt to minimize surface reflections. Seven separate measurements were acquired with the CLBF for each light scatter condition, including the no cell situation. Background fundus illumination and room lighting were kept constant. Subjects were encouraged to blink before each measurement and, if necessary, artificial tears were used to avoid image degradation due to corneal tear film break-up. Laser intensity was maintained on low for all measurements. Axial length was measured using A-scan ultrasound (I^3 Innovative Imaging Inc, Sacramento, CA) to correct for magnification effects due to ametropia. These values were entered into the CLBF database prior to calculation of hemodynamic parameters.

The CLBF allows the operator to use either low (standard) or high laser intensity. In order to investigate the impact of laser intensity on hemodynamic measurements, we also acquired retinal arteriolar hemodynamics both at low and at high intensity laser settings on four of the original ten subjects using the no cell condition (baseline) and the 0.006% and 0.008% microsphere concentration cells.

Statistical Analysis

Repeated measures Analysis of Variance (reANOVA) was used to determine the relationship, if any, between microsphere concentration and each of the hemodynamic parameters i.e. retinal arteriolar diameter, centerline blood velocity and blood flow. For those situations in which a

significant effect was detected by the reANOVA, a Least Squares Difference post-hoc (LSD) comparison test was used to determine the magnitude of artificial light scatter concentration, relative to the no cell condition, that significantly impacted hemodynamic measurements.

The high laser intensity results were compared to the standard laser intensity results for the baseline (i.e. no cell), 0.006% and 0.008% microsphere concentration cell conditions for the same four subjects using repeated measures ANOVA and Tukey HSD post-hoc analysis.

3.3 Results

Group mean (± standard deviation) retinal arteriolar diameter, centerline blood velocity and blood flow as a function of artificial light scatter condition are summarized in Table 3—1. Change of each of the retinal hemodynamic parameters relative to the baseline is shown in Figure 3—2.

Group mean retinal arteriolar diameter and blood flow significantly increased (reANOVA, $p<0.0001$) with increase in microsphere concentration; however, centerline blood velocity was unaffected by artificial light scatter (reANOVA, $p=0.4740$). The LSD post-hoc test revealed that the 0.006% and 0.008% microsphere concentrations produced significantly higher diameter and flow values than the baseline condition (i.e. no cell condition) (Figure 2). Importantly, the water only cell condition produced almost identical values as the baseline for each of the 3 hemodynamic parameters (Table 3—1). The laser tracking system of the CLBF had difficulty stabilizing the laser on to the measurement site for the highest microsphere concentration; for this reason, it was impossible to acquire any measurements on 3 subjects using the 0.008% cell.

Table 3—1. Group mean (± standard deviation) retinal arteriolar diameter, centerline blood velocity and flow as a function of artificial light scatter condition.

	No cell (N=10)	**Water** (N=10)	**0.002%** (N=10)	**0.004%** (N=10)	**0.006%** (N=10)	**0.008%** (N=7)
Diameter (µm)	105.88 (13.47)	105.66 (13.20)	107.67 (13.74)	111.79 (11.14)	120.29 (14.25)	133.18 (14.16)
Velocity (mm/s)	31.61 (8.70)	31.49 (8.53)	32.34 (9.93)	32.02 (8.74)	33.95 (8.79)	33.92 (7.30)
Flow (µl/min)	8.73 (3.72)	8.58 (3.58)	9.21 (4.23)	9.73 (3.92)	11.78 (4.45)	14.54 (4.75)

Figure 3—2 Change in retinal arteriolar diameter (upper), centerline blood velocity (middle) and blood flow (lower) relative to baseline for all cell conditions.

The error bars represent ± 1 standard error of the mean (*; denotes significant difference from baseline i.e. no cell condition).

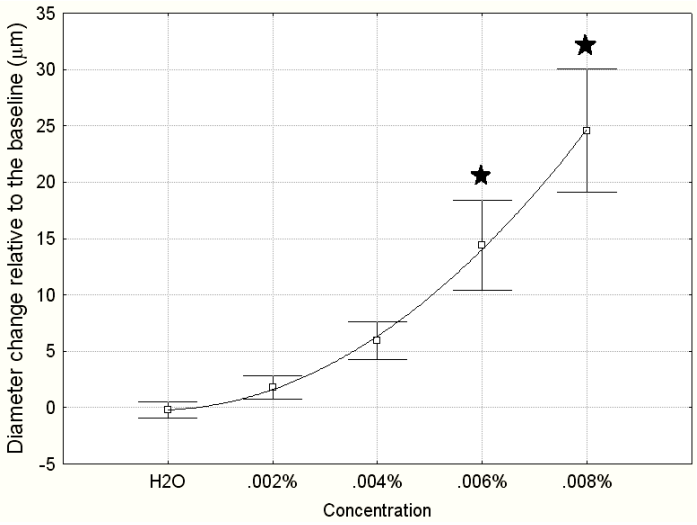

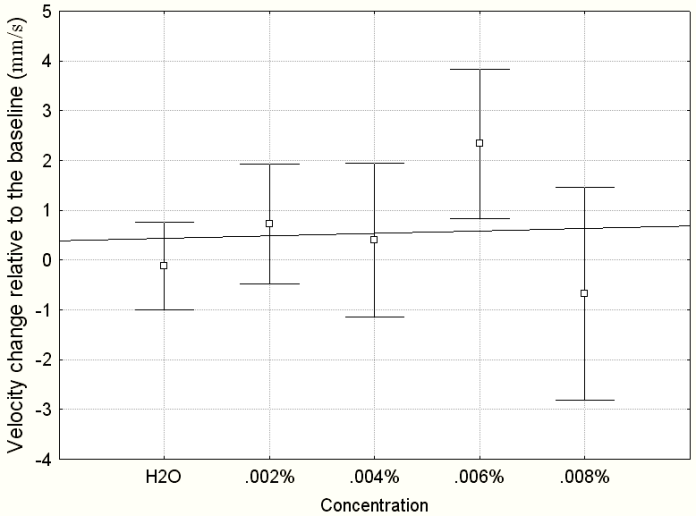

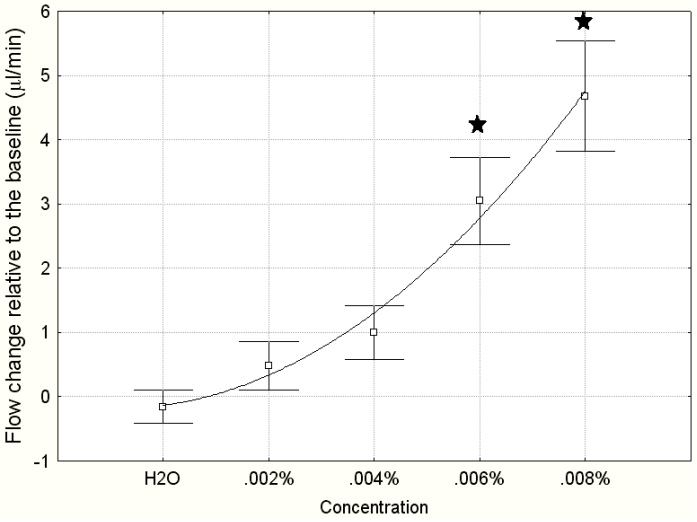

Table 2 and Figure 3 depict the hemodynamic assessment of 4 of the original 10 subjects using both high and low laser intensities. Diameter values attained using the high intensity laser were closer to the baseline; only the 0.008% concentration cell resulted in significantly greater diameter values than the baseline (p=0.0008). Diameter values were significantly less with the high intensity laser setting than the equivalent measurement with the low intensity laser (p=0.0007). Diameter values measured with 0.006% concentration cell were also significantly smaller when the high intensity laser was utilized (p=0.0306). Centerline blood velocity was unaffected by laser intensity (p=0.2817). Similarly, blood flow values attained using high intensity laser were closer to the baseline with only the highest light scatter condition being significantly greater than the baseline (p=0.0313) and were significantly less than the equivalent measurement with the low intensity laser (p=0.0221).

Table 3—2. Group mean (± standard deviation) retinal arteriolar diameter, centerline blood velocity and flow as a function of artificial light scatter condition and laser intensity.

	Low (standard) laser intensity			**High laser intensity**		
	No cell	**0.006%**	**0.008%**	**No cell**	**0.006%**	**0.008%**
	(N=4)	(N=4)	(N=4)	(N=4)	(N=4)	(N=4)
Diameter (µm)	117.76	126.68	141.10	117.68	121.12	129.15
	(9.84)	(13.02)	(6.79)	(10.62)	(12.74)	(9.70)
Velocity (mm/s)	39.52	37.10	38.72	34.37	37.11	36.47
	(7.59)	(7.28)	(10.15)	(9.76)	(10.68)	(9.67)
Flow (µl/min)	13.14	14.51	18.30	11.41	13.24	14.73
	(3.97)	(5.52)	(5.33)	(4.13)	(5.50)	(5.36)

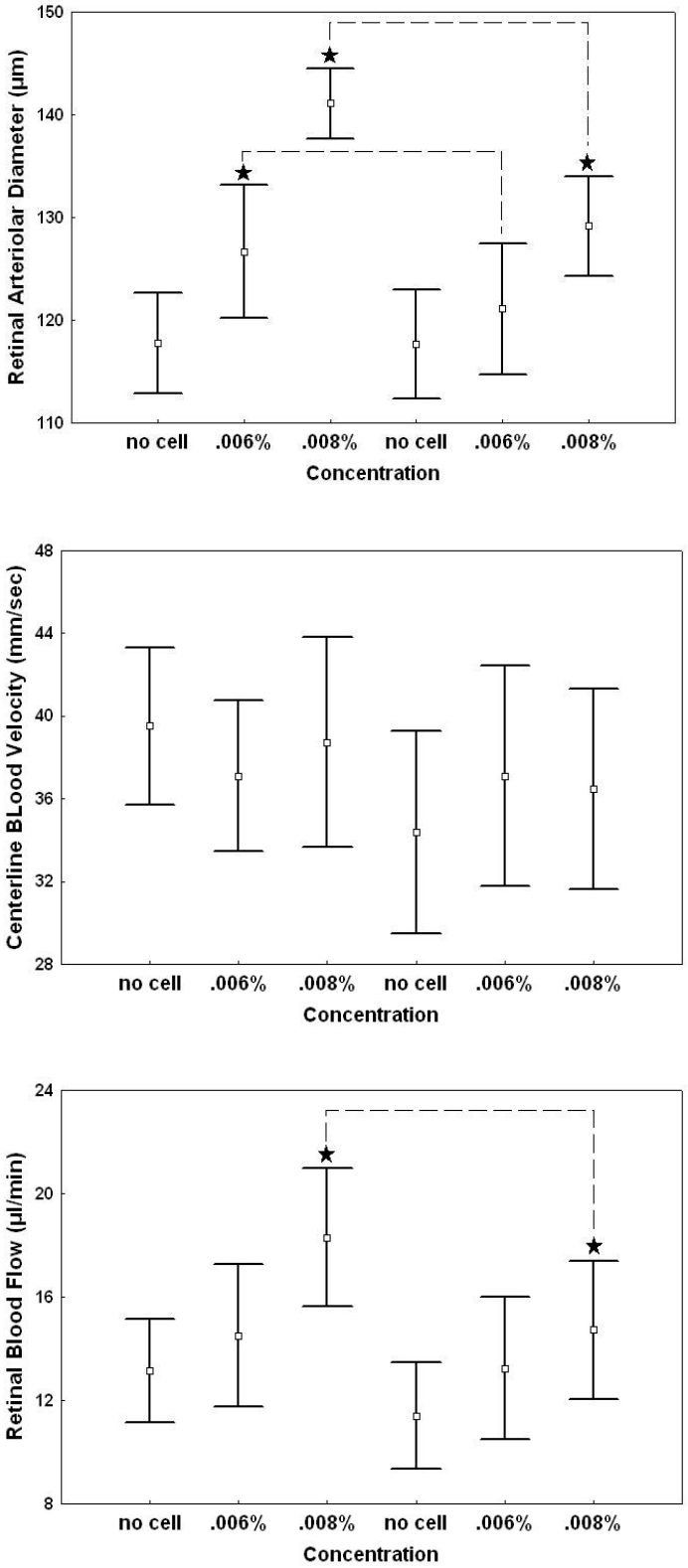

Figure 3—3 Retinal arteriolar diameter (upper), centerline blood velocity (middle) and blood flow (lower) attained at the low (left) and high (right) intensity laser settings for the no cell, 0.006% and 0.008% microsphere concentrations.

The error bars represent ± 1 standard error of the mean (*; denotes significant difference from the baseline. The dashed line denotes a significant difference between identical cell conditions for the low and high laser settings).

3.4 Discussion

Our light scatter model resulted in an artifactual increase of retinal arteriolar diameter ($p<0.0001$) which in turn led to increased derived retinal blood flow values ($p<0.0001$). The increase in blood flow was secondary to the induced change in arteriolar diameter since flow is directly proportional to the second power of diameter, according to the formula used by the CLBF. Centerline blood velocity, however, was not affected by light scatter.

The densitometry technique that is used by the CLBF to measure vessel diameter is increasingly impacted as the magnitude of artificial light scatter increases (Figure 2). We hypothesize that as the light scatter increases, the densitometry image of the vessel looses contrast and the slopes of the densitometry profile broaden (Figure 4). This results in a greater separation of the half-height points causing an artifactual increase in the diameter of the vessel. Ultimately, light scatter will result in breakdown of the CLBF laser tracking system but artifactually increased vessel diameter values can be acquired prior to this point. On the other hand, it is clear that the bidirectional laser Doppler velocimetry technique used to measure centerline blood velocity is robust to the optical effects of artificial light scatter.

Figure 3—4 Densitometry profiles of a vessel measured by the CLBF (left) and schematic representation (right). Upper: baseline (no cell condition). Lower: 0.006% microsphere concentration. DW is the half-height width.

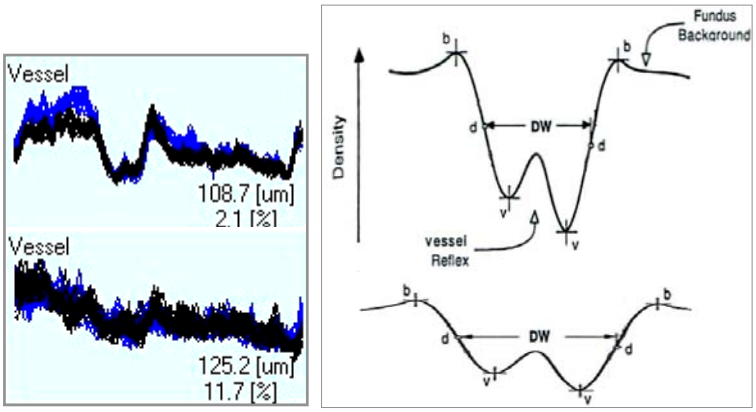

It is apparent that the impact of light scatter upon the densitometric estimation of retinal vessel diameter can, in part, be negated by increasing the intensity of the HeNe laser (Figure 3). Future instrumentation could incorporate a negative feedback loop that automatically increases HeNe laser intensity in situations where the slope of the densitometry profile becomes shallow. In addition, when assessing retinal blood flow in patients with concomitant cataract, we recommend using the high intensity laser setting of the CLBF. CLBF parameters that do not rely on diameter estimation but still provide useful hemodynamic information, such as centerline blood velocity and maximum to minimum velocity ratio, should be given greater attention when assessing retinal blood flow in patients with concomitant cataract.

The data precludes the possibility that a real change in diameter occurred. To explain, if the apparent increase in arteriolar diameter was real then this would be reflected by an increase in blood velocity (since vascular resistance would decrease). The magnitude of apparent increase in arteriolar diameter, if real, would be predicted to result in an increase of blood velocity. An increase in retinal arteriolar diameter of 3.2 ± 1.4 % following hypercapnic provocation resulted in an increase of blood velocity of 26.4 ± 7.0 %[114]. In effect, the finding of an increase in arteriolar diameter in the absence of an increase in blood velocity is contradictory and can only be explained as an artifact of the light scatter cells upon the densitometric estimation of vessel diameter. Furthermore, the magnitude of apparent increase in diameter for the 0.008% light scatter cell is outside the physiological range of diameter change produced by extreme hypercapnic and hyperoxic provocations[17;114].

Are the results of this study only relevant to the limited number of CLBF users worldwide and to those individuals with a specific interest in retinal hemodynamic assessment? A number of techniques designed to assess retinal vessel diameter, including the Retinal Vessel Analyzer[37] and the assessment of retinal photographs used in the Atherosclerosis Risk in Communities Study[120], have been introduced. In particular, recent results from the Atherosclerosis Risk in Communities Study have found that retinal vascular abnormalities are predictive of cardiovascular disease[121]. However, both of these techniques[37;120] use algorithms to assess retinal vessel diameter that are very similar to that used in the CLBF and therefore may be susceptible to artifact resulting from light scatter. Cataract is an inevitable consequence of aging and,

therefore, care needs to be exercised in the interpretation of studies of retinal vessel diameter that utilize cohorts with age as a co-variable.

The results derived from any model, however, need to be interpreted with caution since the model may not accurately simulate the impact of true cataract. From a clinical perspective, we have previously demonstrated the impact of each artificial light scatter condition on fundus visualization achieved with a digital fundus camera that utilizes a polychromatic light source[44;110]. Direct comparison of our artificial light scatter model with a subjective, slit-lamp based cataract grading scale is difficult; however, the magnitude of light scattering medium used in this study is far less than that used to assess confocal optics based instrumentation[44]. Unpublished data from our lab demonstrates that the artificial light scatter model impacts visual acuity and letter contrast sensitivity in a very similar manner to that of nuclear sclerotic cataract. Future work will investigate the impact of light scatter induced by cataract on the retinal blood flow assessments of the quantitative retinal blood flow technique.

4 Assessment of Retinal Hemodynamics in Patients with Cataract

Behrooz Azizi[1,2], Tien Wong[1], Jennifer Wan[2], Shaun Singer[1], Chris Hudson[1,2]

Retina Research Group, [1] Department of Ophthalmology and Vision Science, University of Toronto, Toronto, M5T 2S8; [2] School of Optometry, University of Waterloo, Waterloo, N2L 3G1; Ontario, CANADA.

	Concept / Design	Recruitment	Acquisition of data	Analysis	Write-up / publication
Azizi	X	X	X	X	X
Wong			X		
Wan		X	X		
Singer		X			
Hudson	X			X	X

Table detailing role of each author in this publication (X denotes significant contribution)

4.1 Introduction

Disturbance of retinal blood flow is a feature of many ocular diseases[1;117], including diabetic retinopathy[1;11;22;35;117], age-related maculopathy[28], and a subset of patients with glaucoma[21;27]. Retinal hemodynamic assessment has the potential to play a role in the early detection and monitoring of some of these diseases[22], as well as evaluating the retinal vascular response to surgical and drug treatments[21]. There are techniques available that permit the non-invasive quantification of retinal hemodynamics. One such instrument is Canon Laser Blood Flowmeter (CLBF) used to assess retinal blood flow in real units (μl/min), derived from simultaneously measuring vessel diameter (μm) and centerline blood velocity (mm/sec) [10;53;55]. The impact of lens opacity on the assessment of retinal blood flow using the CLBF has never been studied, despite the fact that it has been used widely in elderly subjects where concomitant existence of cataract or intraocular light scatter is inevitable.

Recent work from our group has shown that the densitometry technique that is used by a number of techniques to measure vessel diameter, including the CLBF, is increasingly impacted as the magnitude of artificial light scatter increases, resulting in artifactually elevated diameter and blood flow measurements[122]. The present study was designed to further investigate these findings in patients with intra-ocular light scatter induced by cataract.

4.2 Methods

Thirty patients scheduled for extracapsular cataract extraction using phacoemulsification and intraocular lens implantation were prospectively recruited. Ten patients met all the inclusion and exclusion criteria and were included in the analysis. Subjects were between the ages of 61 and 84 years (mean age 73 years, SD 8). Subjects had no corneal abnormalities, including dry eye, scarring, dystrophy, and corneal transplant. Patients with post operative complications were excluded from the study. All volunteers were informed about the details of the study and gave their consent to participate. The research followed the tenets of the Declaration of Helsinki and was approved by the Research Ethics Board of the University Health Network and also by the Office of Research Ethics of the University of Waterloo.

Quantitative Assessment of Retinal Arteriolar Blood Flow

The quantitative assessment of retinal blood flow was undertaken using the Canon Laser Blood Flowmeter (CLBF), model 100. The CLBF utilizes bidirectional laser Doppler velocimetry (LDV) to quantify the centerline blood velocity in the large retinal vessels (Figure 1), densitometry to measure vessel diameter (Figure 2) and an image stabilization system to minimize the impact of eye movement[21;45]. The details of the CLBF have been published by our group [17;122] and numerous other groups[41;45;49;55] previously.

Velocity measurements are acquired automatically every 0.02secs throughout the 2secs measurement window, resulting in a velocity-time trace that depicts the systolic-diastolic variation of blood velocity.

Diameter measurements are acquired every 4msecs during the first and last 60msecs of the 2 second velocity acquisition window.

Magnification effects associated with refractive and axial components of ametropia are corrected to provide absolute measurements of diameter (μm), velocity (mm/sec) and flow (μL/min).

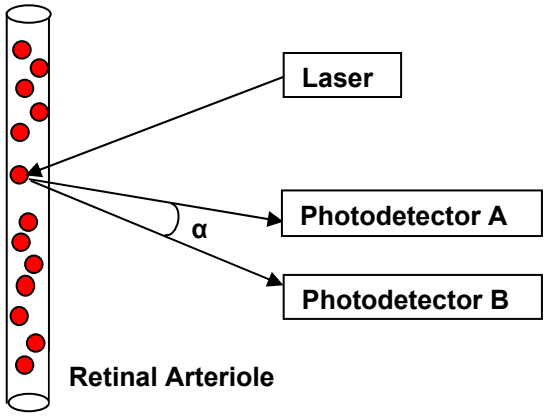

Figure 4—1 Bidirectional laser Doppler Velocimetry. A red diode laser (675nm, 80μm x 50 μm oval) is used to acquire bi-directional LDV measurements. The frequency shift of the light scattered by the moving blood cells at the illuminated site is simultaneously focused by two distinct photodetectors separated from each other by a fixed, known angle[41]. The maximum frequency shift detected by each photo-detector is subtracted to allow the absolute quantification of centerline blood velocity, irrespective of the angle between the moving particle and reflected beam[49;118]. The resulting Doppler signal is analyzed using a previously described algorithm[49]; the frequency shift is determined as the frequency at which there is an abrupt reduction in the amplitude of the fluctuations in the Doppler-shift power spectrum. This determination does not depend on any presumed shape of the average power spectral density curve.

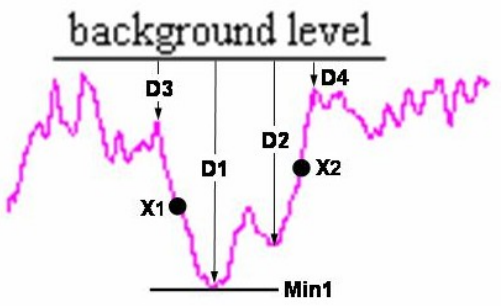

Figure 4—2 Retinal vessel diameter is determined by projecting a rectangular (1500 μm x 150 μm) green (543 nm) HeNe diode laser perpendicular to the vessel segment measurement site. Densitometry analysis of the cross-sectional vessel image on the CLBF array sensor is used to calculate vessel diameter. The minimum point (Min_1) in the central portion of the image is designated as the nominal vessel center with D_1 being its signal level from the background level. When mirror reflection occurs from the vessel wall, the second minimum point is observed in the neighborhood of Min_1 with signal level D_2. The maximum points on either side are detected as the vessel edges with D_3 and D_4 signal levels. The half height points (X_1 and X_2) are points on the image whose signal levels are $(D_1+D_3)/2$ and $(D_2+D_4)/2$, respectively. The width between X_1 and X_2 is taken to represent the uncorrected vessel diameter and is converted into micron units after correction for axial and refractive magnification effects[45;119]. (Image courtesy of Canon Inc, Japan)

Procedures

Two visits were required to complete the study, one prior to the surgery and one at least six weeks after the surgery to allow for a level of post-operative recovery that would not hinder retinal imaging. The severity of cataract was documented using the Lens Opacity Classification System[90] (LOCS, III) on the pre-operative visit. Each subject underwent the assessment of intraocular light scatter status at both visits using logMAR ETDRS visual acuity charts (10% & 90% contrast) and the Brightness Acuity Tester (BAT) at high and low illumination settings. The charts were illuminated to 100cdm^{-2} and the recommended viewing distance of 4 meters was employed. A "by-letter" scoring system was utilized that gave credit to each correct letter[123]. The order of chart presentation was randomized to minimize any familiarity that patients may gain of the letter composition of the charts. The eye to undergo surgery was dilated using Mydriacyl 1% (Alcon Canada Inc. Mississauga, Canada).

Retinal arteriolar hemodynamics were measured in the superior temporal arteriole. The measurement site was selected in a relatively straight vessel segment, distant from any bifurcations and within 1 disc diameter of the optic nerve head. Retinal hemodynamic measurements were then acquired at the same measurement site post-operatively, with the aid of the fixation target memory feature of the CLBF. Seven to ten separate measurements were acquired with the CLBF at each visit. The CLBF allows the operator to use either low (standard) or high intensity HeNe laser. Based on our previous study[122], the high laser intensity setting was utilized pre- and post-operatively to aid retinal visualization through cataract and to reduce impact of light scatter on the estimation of retinal vessel diameter. Background camera illumination and room lighting were kept constant between visits. Subjects were encouraged to blink before each measurement and, if necessary, artificial tears were used to avoid image degradation due to corneal tear film break-up. Axial length was measured using IOLMaster (Carl Zeiss Meditec) to correct for magnification effects due to ametropia. These values were entered into the CLBF database prior to calculation of hemodynamic parameters.

Statistical Analysis

The Wilcoxon signed-rank test was used to compare each of the hemodynamic parameters i.e. retinal arteriolar diameter, centerline blood velocity and blood flow, pre- and post-operatively, because the data was not normally distributed. All analyses were performed using SPSS 16.0.

4.3 Results

Ten of the original thirty patients were included in the analysis. Twelve of the patients were impossible to image as the cataract was very dense and the laser tracking system of the CLBF had difficulty stabilizing the laser on to the measurement site, five were lost to follow up, two cancelled their surgeries, and one had inadequate post-op pupil dilation who were excluded from the study.

Change in group mean retinal arteriolar diameter, centerline blood velocity and blood flow pre- and post-operatively are summarized in Table 1, while scatter plots showing the change of individual data post-operatively are shown in Figure 3. Group mean retinal arteriolar diameter and blood flow significantly decreased post-operatively (Wilcoxon, $p=0.022$ and $p=0.028$ respectively). However, centerline blood velocity was unchanged (Wilcoxon, $p=0.074$) post-operatively.

Severity of cataract is recorded in Table 2, using the Lens Opacity Classification System (LOCS, III). Table 3 depicts changes in logMAR visual acuity as an assessment of intra-ocular light scatter (glare) achieved by subtracting the logMAR VA between high and low illumination settings on BAT. Both 10% and 96% contrast ETDRS charts were used. None of the differences were significant as the numbers were limited ($n=9$), and all the changes are positive as expected since there is more glare using high compared to low illumination. We expected to see a higher glare pre-operatively, which was the case using the 96% but not the 10% contrast chart (differences are not statistically significant).

Table 4—1 Group mean ± standard deviation (Median) retinal arteriolar diameter, centerline blood velocity and flow pre- and post-operatively (i.e. cataract and IOL, respectively) (IOL; intra-ocular lens).

	Diameter [µm]	**Velocity [mm/s]**	**Flow [µl/min]**
Cataract [n=10]	120.54 ± 20.52 (114.70)	39.38 ± 8.26 (38.16)	14.15 ± 6.91 (11.46)
IOL [n=10]	106.23 ± 5.69 (108.27)	35.39 ± 9.00 (37.02)	9.50 ± 2.70 (10.20)

Table 4—2 LOCS III system used to document the severity of cataract. Nuclear opalescence (NO), nuclear color (NC), cortical opacity (CO), post subcapsular (PS).

LOCS III:	**NO**	**NC**	**CO**	**PS**
Mean	3.1	2.6	2.9	1.4
SD	0.7	0.7	0.7	0.6

Table 4—3 Assessment of intra-ocular light scatter: Change in logMAR visual acuity between the high and low illumination settings of the Brightness Acuity Tester (BAT) using 10% and 96% contrast ETDRS charts.

		Δ logMAR VA	
		10%	**96%**
Cataract	Mean	0.11	0.06
	SD	0.12	0.14
IOL	Mean	0.19	0.11
	SD	0.15	0.10

Figure 4—3 Boxplot (left) and Scatterplot (right) of each individual showing the retinal arteriolar diameter (upper), centerline blood velocity (middle), and blood flow (lower) measured pre- (i.e. cataract) and post-operatively (i.e. IOL). (IOL; intra-ocular lens).

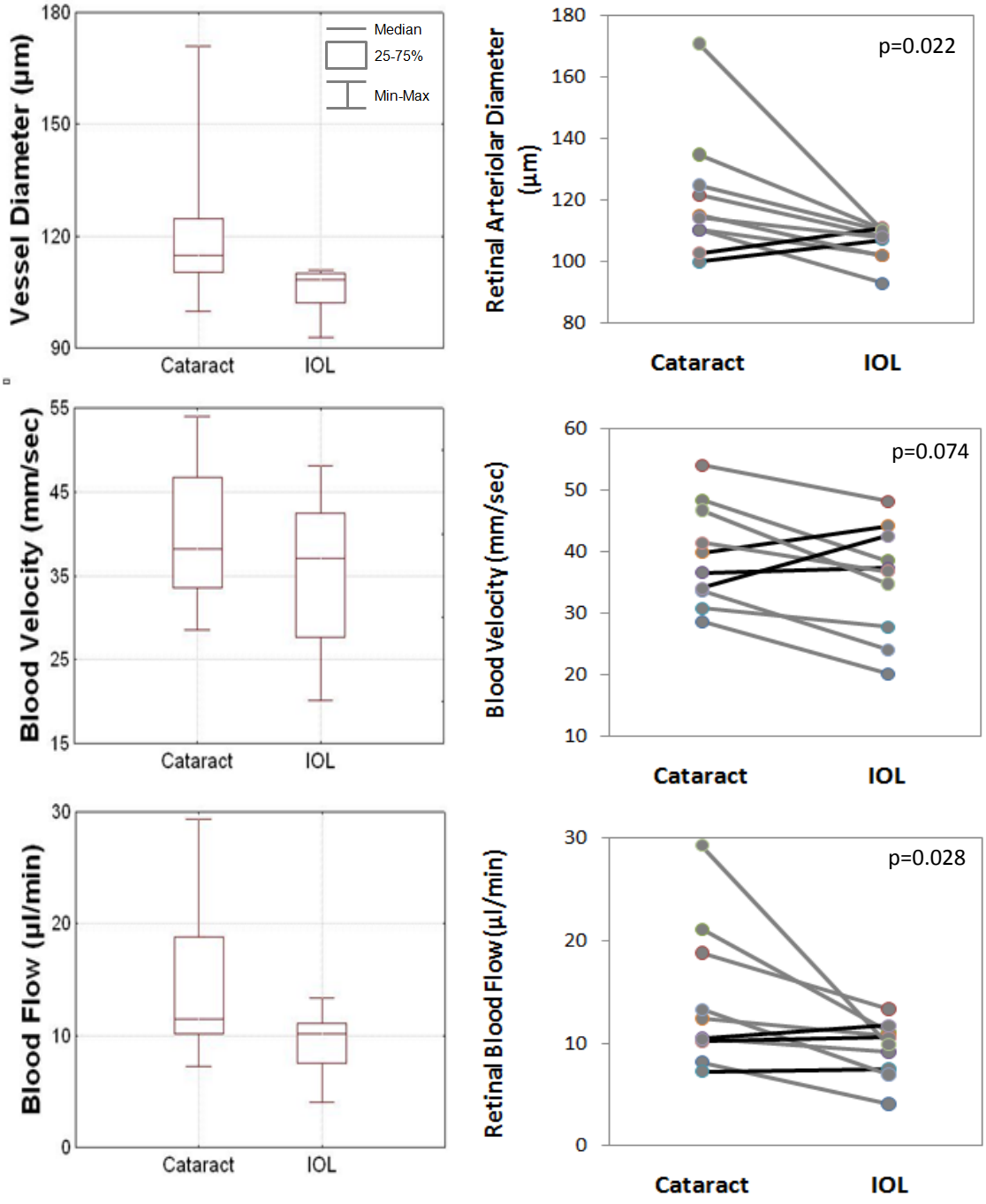

4.4 Discussion

Retinal arteriolar diameter was artifactually elevated in the presence of cataract ($p<0.022$) which in turn led to an increase of the derived retinal blood flow values ($p<0.028$). The increase in blood flow was secondary to the induced change in arteriolar diameter since flow is directly proportional to the second power of diameter. Centerline blood velocity, however, was not significantly affected by light scatter produced by cataract. These findings are in close agreement with those of our earlier study using simulated light scatter [122].

The densitometry technique that is used by the CLBF to measure vessel diameter is impacted by the light scatter induced by cataract. In our previous publication, we hypothesized that as simulated light scatter increased, the densitometry image of the vessel lost contrast and the slopes of the densitometry profile broadened. Figure 4 illustrates this effect. Ultimately, light scatter will result in breakdown of the CLBF laser tracking system but artifactually increased vessel diameter values can be acquired prior to this point. On the other hand, it is clear that the bidirectional laser Doppler velocimetry technique used to measure centerline blood velocity is relatively robust to the optical effects of artificial light scatter, although the data does reveal a trend (Wilcoxon, $p=0.074$) for increased velocity in the presence of cataract.

In our previous study[122], we showed that using the high intensity laser setting of the CLBF reduced the impact of light scatter on the measured diameter values. Nevertheless, we have demonstrated in this study that using the high intensity laser setting of the CLBF still results in erroneous hemodynamic measurements in the presence of cataract. The use of the high laser setting was necessary in order to allow adequate visualization of the fundus and proper functioning of the laser tracking system of the CLBF.

CLBF parameters that do not rely on diameter estimation may still provide useful hemodynamic information, such as centerline blood velocity and maximum-to-minimum velocity ratio, should be given greater attention when assessing retinal blood flow in patients with concomitant cataract.

The data precludes the possibility that a real change in diameter occurred following phacoemulcification and IOL implantation. To explain, if the apparent reduction in arteriolar diameter after surgical removal of the cataract was real then this would be reflected by a decrease in blood velocity (since vascular resistance would increase as a result of any true vasoconstriction). Furthermore, the magnitude of apparent change in diameter after surgical removal of cataract is outside the physiological range of diameter change produced by extreme hypercapnic and hyperoxic provocations [17;114].

A number of techniques designed to assess retinal vessel diameter, including the Retinal Vessel Analyzer[37] and the assessment of retinal photographs[120], have been utilized. However, both of these techniques[37;120] use algorithms to assess retinal vessel diameter that are very similar to that used in the CLBF and therefore may be susceptible to artifact resulting from light scatter. We showed significant change in retinal vessel diameter measurements of patients with mild to moderate cataract (Table 2). Cataract is an inevitable consequence of aging, therefore, care needs to be exercised in the interpretation of studies of retinal vessel diameter that utilize cohorts with age as a co-variable.

Our analysis of intra-ocular light scatter using BAT and ETDRS charts (10% and 96% contrast) did not result in any statistically significant difference pre- and post-operatively. This could be explained by the low number of patients. Patients' pupils were also dilated at the time of examination which could improve their vision prior to the surgery minimizing the difference pre- and post-operatively.

5 Conclusions

Retinal hemodynamic assessment is a promising approach to study the pathophysiology of the ocular diseases and has the potential to play a key role in early diagnosis as there is increasing evidence that vascular pathologies play a pivotal role in the etiology and progression of number of ophthalmic diseases, including glaucoma, age-related macular degeneration, and diabetic retinopathy[2;20;21]. Our laboratory has shown reduced retinal vascular reactivity in diabetic patients[22-25]. Studies in glaucoma patients have shown reduced blood flow to the retinal ganglion cells and optic nerve, possibly contributing to the damage seen in glaucomatous optic neuropathy[21;26;27]. Changes in macular retinal capillary blood flow are also documented in age-related maculopathy[28].

There are number of novel instruments developed to assess retinal hemodynamics. Impact of lenticular opacity have been widely neglected despite the wide use of these instruments in the elderly population when increase in the intraocular light scatter is often observed and concomitant cataract is inevitable. In order to investigate the impact of intra-ocular light scatter on the CLBF, we first used a simulated light scatter model and subsequently proved our findings using real cataract patients, pre and post operatively.

Our light scatter model resulted in an artifactual increase of retinal arteriolar diameter ($p<0.0001$) which in turn led to increased retinal blood flow values ($p<0.0001$). Centerline blood velocity, however, was not affected by the simulated light scatter. In our second study, retinal arteriolar diameter was similarly elevated in the presence of cataract ($p<0.022$) which in turn led to an increase of the derived retinal blood flow values ($p<0.028$). Centerline blood velocity was not significantly affected by light scatter produced by cataract similar to our findings in the first study using simulated light scatter.

The densitometry technique that is used by the CLBF to measure vessel diameter is impacted by the light scatter induced by cataract. We hypothesize that as light scatter increases, the densitometry image of the vessel loses contrast and the slopes of the densitometry profile broaden. Ultimately, light scatter will result in breakdown of the CLBF laser tracking system but artifactually increased vessel diameter values can be acquired prior to this point. On the other

hand, it is clear that the bidirectional laser Doppler velocimetry technique used to measure centerline blood velocity is relatively robust to the optical effects of artificial light scatter, although the data does reveal a trend (Wilcoxon, p=0.074) for increased velocity in the presence of cataract.

In our first study, we showed that using the high intensity laser setting of the CLBF reduced the impact of light scatter on the measured diameter values. Nevertheless, we have demonstrated in our second study that using the high intensity laser setting of the CLBF still results in erroneous hemodynamic measurements in the presence of cataract. The use of the high laser setting was necessary in order to allow adequate visualization of the fundus and proper functioning of the laser tracking system of the CLBF prior to surgery.

A number of techniques designed to assess retinal vessel diameter, including the Retinal Vessel Analyzer[37] and the assessment of retinal photographs[120], use algorithms that are very similar to that used in the CLBF and therefore may be susceptible to artifact resulting from light scatter. Cataract is an inevitable consequence of aging and we showed significant change in retinal vessel diameter measurements of patients with mild to moderate cataract. Therefore, care needs to be exercised in the interpretation of studies of retinal vessel diameter that utilize cohorts with age as a co-variable.

Future instrumentation could incorporate a negative feedback loop that automatically increases HeNe laser intensity in situations where the slope of the densitometry profile becomes shallow. Other instruments such as the new generation of the Stray Light Meter, developed by Van den Burg et al [100;102], could also be incorporated into the CLBF and other instruments to allow for a quick measurement of patients' intraocular light scatter on each visit. This measure of the intraocular light scatter could be compared with previous readings and in case of any change, the instrument could automatically adjust the laser settings or use a mathematical model to correct the measured retinal vessel diameter and subsequently blood flow. Another way of dealing with the impact of intraocular light scatter change is to use other CLBF parameters that do not rely on diameter estimation but still provide useful hemodynamic information, such as centerline blood velocity and maximum to minimum velocity ratio.

References

1. Lemp M, Wolfley D. Alder's Physiology of the Eye: Clinical Application. St. Louis, USA: Mosby Year Book,1992.

2. Harris A, Jonescu-Cuypers CP, Kagemann L, Ciulla TA, Krieglstein GK. Atlas of ocular blood flow: vascular anatomy, pathophysiology, and metabolism. Philadelphia: Butterworth-Heinemann (Elsevier),2003.

3. Pournaras C, Donati G. In: Albert D, JF (eds) *Principles and Practice of Ophthalmology.* W.B. Saunders Co, 2000.

4. Snell RS, Lemp MA. Clinical Anatomy of the Eye. Malden, MA, USA: Blackwell Science,1998.

5. Bhutto I, Lutty G. In: Shepro D (ed) *Microvascular Research*. Boston: Elsevier Academic Press, 2006.

6. Reamington L. *Clinical Anatomy of the Visual System*. Boston: Butterworth-Heineman, 1998.

7. Feke GT, Tagawa H, Deupree DM, Goger DG, Sebag J, Weiter JJ. Blood flow in the normal human retina. *Invest Ophthalmol.Vis.Sci.* 1989:**30**: 58-65.

8. Baker M, Wayland H. On-line volume flow rate and velocity profile measurement for blood in microvessels. *Microvasc.Res.* 1974:**7**: 131.

9. Schmid-Schoenbein G, Zweifach B. RBC velocity profiles in arterioles and venules of the rabbit omentum. *Microvasc.Res.* 1975:**10**: 153.

10. Guan K, Hudson C, Flanagan JG. Variability and repeatability of retinal blood flow measurements using the Canon Laser Blood Flowmeter. *Microvasc.Res.* 2003:**65**: 145-151.

11. Hayreh SS. Blood Flow in the Optic Nerve Head and Factors that may Influence it. *Progress in Retinal & Eye Research* 2001:**20**: 595-624.

12. Georgia State University. HyperPhysics. http://hyperphysics.phy-astr.gsu.edu . 2005. 1-1-2005.

13. Riva CE, Titze P, Hero M, Petrig BL. Effect of acute decreases of perfusion pressure on choridal blood flow in humans. *Investigative Ophthalmology and Visual Science* 1997:**38**: 1752-1760.

14. Riva CE, Titze P, Hero M, Movaffaghy A, Petrig BL. Choroidal blood flow during isometric exercises. *Investigative Ophthalmology and Visual Science* 1997:**38**: 2338-2343.

15. Lovasik J, V, Kergoat H, Riva CE, Petrig BL, Geiser M. Choroidal Blood Flow during Exercise-Induced Changes in the Ocular Perfusion Pressure. *Invest.Ophthalmol.Vis.Sci.* 2003:**44**: 2126-2132.

16. Dorner GT, Garhoefer G, Zawinka C, Kiss B, Schmetterer L. Response of retinal blood flow to CO2-breathing in humans. *Eur.J Ophthalmol.* 2002:**12**: 459-466.

17. Gilmore E, Hudson C, Preiss D, Fisher JA. Retinal arteriolar diameter, blood velocity and blood flow response to an isocapnic hyperoxic provocation. *Am J Physiol-Heart Circ Physiol* 2005:**288**: H2912-H2917.

18. Jean-Louis S, Lovasik JV, Kergoat H. Systemic hyperoxia and retinal vasomotor responses. *Invest Ophthalmol.Vis Sci* 2005:**46**: 1714-1720.

19. Jeppesen P, Sanye-Hajari J, Bek T. Increased blood pressure induces a diameter response of retinal arterioles that increases with decreasing arteriolar diameter. *Invest Ophthalmol.Vis Sci* 2007:**48**: 328-331.

20. Harris A, Kagemann L, Ehrlich R, Rospigliosi C, Moore D, Siesky B. Measuring and interpreting ocular blood flow and metabolism in glaucoma. *Can.J Ophthalmol.* 2008:**43**: 328-336.

21. Harris A, Kagemann L, Cioffi GA. Assessment of human ocular hemodynamics. *Surv.Ophthalmol.* 1998:**42**: 509-533.

22. Guan K, Hudson C, Wong T *et al.* Retinal hemodynamics in early diabetic macular edema. *Diabetes* 2006:**55**: 813-818.

23. Gilmore ED, Hudson C, Nrusimhadevara RK *et al.* Retinal arteriolar hemodynamic response to a combined isocapnic hyperoxia and glucose provocation in early sight-threatening diabetic retinopathy. *Invest Ophthalmol.Vis Sci* 2008:**49**: 699-705.

24. Gilmore ED, Hudson C, Nrusimhadevara RK *et al.* Retinal arteriolar hemodynamic response to an acute hyperglycemic provocation in early and sight-threatening diabetic retinopathy. *Microvasc.Res.* 2007:**73**: 191-197.

25. Gilmore ED, Hudson C, Nrusimhadevara RK *et al.* Retinal arteriolar diameter, blood velocity, and blood flow response to an isocapnic hyperoxic provocation in early sight-threatening diabetic retinopathy. *Invest Ophthalmol.Vis Sci* 2007:**48**: 1744-1750.

26. Flammer J, Orgul S, Costa VP *et al.* The impact of ocular blood flow in glaucoma. *Prog.Retin.Eye Res.* 2002:**21**: 359-393.

27. Hayreh SS. The blood supply of the optic nerve head and the evaluation of it - myth and reality. *Progress in Retinal & Eye Research* 2001:**20**: 563-593.

28. Holger R, Christoph WS, Lang GK, Gabriele E.Lang. Changes of retinal capillary blood flow in age-related maculopathy. *Graefe's Archive for Clinical and Experimental Ophthalmology* 2000:**238**: 960-964.

29. Silver DM, Farrell RA, Langham ME, O'Brien V, Schilder P. Estimation of pulsatile ocular blood flow from intraocular pressure. *Acta Ophthalmol.Suppl* 1989:**191**: 25-29.

30. Silver DM, Farrell RA. Validity of pulsatile ocular blood flow measurements. *Surv.Ophthalmol.* 1994:**38 Suppl**: S72-S80.

31. Silver DM, Geyer O. Pressure-volume relation for the living human eye. *Curr.Eye Res.* 2000:**20**: 115-120.

32. Schmetterer L, Lexer F, Unfried C, et al. Topical measurement of fundus pulsations. *Optl Eng* 1995: 711-716.

33. Hickam JB, Frayser R. Aphotographic method for measuring the mean retinal circulation time using fluorescein. *Invest Ophthalmol.* 1965:**4**: 876-884.

34. Harris A, Kagemann L, Ciulla TA, Kumar R. Angiographic Assessment. In: Ciulla TA, Regillo CD, Harris A (eds) *Retina and Optic Nerve Imaging*. Philadelphia, USA: Lippincott Williams & Wilkins, 2003.

35. Schmetterer L, Wolzt M. Ocular blood flow and associated functional deviations in diabetic retinopathy. *Diabetologia* 1999:**42**: 387-405.

36. Wolf S, Arend O, Toonen H, Bertram B, Jung F, Reim M. Retinal capillary blood flow measurement with a scanning laser ophtalmoscope. *Ophthalmology* 1991:**98**: 996-1000.

37. Munch K, Vilser W, Senff I. Adaptive algorithm for automatic measurement of retinal vascular diameter. *Biomed.Tech.(Berl).* 1995:**40**: 322-325.

38. Polak K, Dorner G, Kiss B *et al.* Evaluation of the Zeiss retinal vessel analyser. *Br.J Ophthalmol.* 2000:**84**: 1285-1290.

39. Orge FH, Harris A, Ciulla TA, Rechtman E, McNulty L. Color Doppler Imaging. In: Ciulla TA, Regillo CD, Harris A (eds) *Retina and Optic Nerve Imaging*. Philadelphia, USA: Lippincott Williams & Wilkins, 2003.

40. Lieb WE, Cohen SM, Merton DA, Shields JA, Mitchell DG, Goldberg BB. Color Doppler imaging of the eye and orbit. Technique and normal vascular anatomy. *Arch.Ophthalmol.* 1991:**109**: 527-531.

41. Feke GT, Yoshida A, Schepens CL. Laser Based Instruments for Ocular Blood Flow Assessment. *Journal of Biomedical Optics* 1998:**3**: 415-422.

42. Petrig BL, Riva CE, Hayreh SS. Laser Doppler flowmetry and optic nerve head blood flow. *American Journal of Ophthalmology* 1999:**127**: 413-425.

43. Kagemann L, Harris A, Siesky BA. Laser Doppler flowmetry: the Heidelberg Retina Flowmeter. In: Ciulla TA, Regillo CD, Harris A (eds) *Retina and Optic Nerve Imaging*. Philadelphia, USA: Lippincott Williams & Wilkins, 2003.

44. Venkataraman ST, Hudson C, Harvey E, Flanagan JG. Impact of simulated light scatter on scanning laser Doppler flowmetry. *Br.J.Ophthalmol.* 2005:**89**: 1192-1195.

45. Kagemann L, Harris A, Kumar R, Rechtman E. New technologies for the assessment of retinal circulation. In: Ciulla TA, Regillo CD, Harris A (eds) *Retina and Optic Nerve Imaging*. Philadelphia, USA: Lippincott Williams & Wilkins, 2003.

46. Damon DN, Duling DR. A comparison between mean blood velocities and centerline red cell velocities as measured with a mechanical image streeking velocimeter. *Microvascular Res* 1979:**17**: 330-332.

47. Feke, Gilbert T., Ishiko, S., and McMeel, J. W. Evaluation of a new laser Doppler retinal blood flowmeter. Invest.Ophthalmol.Vis.Sci. 40, S487(ARVO abst 2570). 1999.

48. Riva CE, Grunwald JE, Sinclair SH. Laser Doppler measurement of relative blood velocity in the human optic nerve head. *Invest Ophthalmol.Vis Sci* 1982:**22**: 241-248.

49. Feke GT, Goger DG, Tagawa H, Delori FC. Laser Doppler technique for absolute measurement of blood speed in retinal vessels. *IEEE Trans.Biomed.Eng.* 1987:**34**: 673-680.

50. Feke GT, Delori FC, Webb RH. Beam steering optical system and method and ophthalmic apparatus using same having spaced apart irradiation and observation paths. *US Patent No.* 1997:**5**: 633-695.

51. Kagemann L, Harris A, Jonescu-Cuypers CP, et al. Comparison of ocular hemodynamics measured by a new retinal flowmeter and color Doppler imaging. *Ophthalimic Surg lasers* 2001:**34**.

52. Garcia JP, Jr., Garcia PT, Rosen RB. Retinal blood flow in the normal human eye using the canon laser blood flowmeter. *Ophthalmic Res.* 2002:**34**: 295-299.

53. Yoshida A, Feke GT, Mori F *et al.* Reproducibility and clinical application of a newly developed stabilized retinal laser Doppler instrument. *Am.J Ophthalmol.* 2003:**135**: 356-361.

54. Geiser M, Logean E, Petrig BL. Reproducibility and clinical application of a newly developed stabilized retinal laser Doppler instrument. *Am.J Ophthalmol.* 2003:**136**: 583-584.

55. Nagaoka T, Mori F, Yoshida A. Retinal artery response to acute systemic blood pressure increase during cold pressure test in humans. *Invest.Ophthalmol.Vis.Sci.* 2002:**43**: 1941-1945.

56. World Health Organization. Magnitude and causes of visual impairment. http://www.who.int/mediacenter/factsheets/fs282/en/ . 2004. 6-9-2005.

57. World Health Organization. Preservation and Restoration of Vision: Initiatives and Resources. http://www.icoph.org/prev/index.html#loss . 2005. 6-9-2005.

58. Hennelly ML, Barbur JL, Edgar DF, Woodward EG. The effect of age on the light scattering characteristics of the eye. *Opthalmic and Physiological Optics* 1998:**18**: 197-203.

59. Thaung J, Sjöstrand J. Integrated light scattering as a function of wavelength in donor lenses. *Journal of the Optical Society of America* 2002:**19**: 152-157.

60. Van Den Berg T, Ijspeert JK. Light Scattering in Donor Lenses. *Vision Research* 1995:**35**: 169-177.

61. Siik, S. Lens autofluorescence in ageing and cataractous human lenses; clinical applicability. 1999. Department of Ophthalmology, University of Oulou .

62. Whitaker D, Steen R, Elliot DB. Light scatter in the normal young, elderly and cataractous eye demonstrates little wavelength dependency. *Optometry and Vision Science* 1993:**70**: 963-968.

63. van den Berg TJ, Tan KEWP. Light transmittance of the human cornea from 320 to 700 nm for different ages. *Vision Research* 1994:**34**: 1453-1456.

64. Hood BD, Garner B, Truscott RJW. Human Lens Coloration and Aging . *J Biol Chem* 1999:**274**: 32547-32550.

65. Weale R. *Mechanisms of cataract formation in the human lens*. London: Academic Press,1981.

66. Siik S, Airaksinen PJ, Tuulonen A, Alanko HI, Nieminen H. Lens autofluorescence in healthy individuals. *Acta Ophthalmol (Copenh)* 1991:**69**: 187-192.

67. Thomson D. Managing cataracts in the optometric practice. *Optician* 2003:**225**.

68. Thomson D. Methods of assessing cataract and the effect of opacities on vision. *Optometry Today* 2001:**41**: 26-30.

69. Ocampo, V. V. D. and Foster, S. C. Senile Cataract. http://emedicine.medscape.com/article/1210914-overview . 5-20-2009. 12-1-2009.

70. Lawrenson JG. Age-related cataract: Epidemiology, pathogenesis and management. *Optometry today* 2003:**43**: 24-28.

71. Graw J. Congenital hereditary cataracts. *International Journal of Developmental Biology* 2004:**48**: 1031-1044.

72. Armstrong RA. Genetics of catact. *Optometry today* 2005: 25-27.

73. Reddy MA, Francis PJ, Berry V, Bhattacharya SS, Moore AT. Molecular genetic basis of inherited cataract and associated phenotypes. *Surv.Ophthalmol.* 2004:**49**: 300-315.

74. Ruotolo R, Grassi F, Percudani R *et al.* Gene expression profiling in human age-related nuclear cataract. *Mole.Vision* 2003:**9**: 538-548.

75. Haws J, Heijmancik J, Huang OL *et al.* Identification and functional clustering of global gene expression differences between human age-related cataract and clear lenses. *Mole.Vision* 2003:**9**: 515-537.

76. Dolin PJ. Ultraviolet radiation and cataract: a review of the epidemiological evidence. *Br J Ophthalmol* 1994:**78**: 478-482.

77. Zigman S. Ultraviolet A and cataracts: basic research and practical applications. *International Ophthalmology Clinics* 2005:**45**: 29-40.

78. Wegener A, Landwehr H, Laser H, et al. Interactive effects of nutritional deficiencies on UV damage to the cornea and lens in the Brown Norway rat. *Investigative Ophthalmology and Visual Science* 1998:**39(Suppl)**: S318.

79. West SK. Smoking and the risk of eye disease. In: A.Taylor (ed) *Nutritional and environmental influences on the eye*. Florida: CRC Press, 1999.

80. Lindblad BE, Hakansson N, Svensson H, Philipson B, Wolk A. Intensity of Smoking and Smoking Cessation in Relation to Risk of Cataract Extraction: A Prospective Study of Women. *Am.J.Epidemiol.* 2005:**162**: 73-79.

81. Krishnaiah S, Vilas K, Shamanna BR, Rao GN, Thomas R, Balasubramanian D. Smoking and its association with cataract: results of the Andhra Pradesh eye disease study from India. *Investigative Ophthalmology & Visual Science* 2005:**46**: 58-65.

82. Brown NP. Mechanisms of cataract formation. *Optometry today* 2001:**41**: 27-31.

83. Leske MC, Wu SY, Hennis A, Connell AM, Hyman L, Schachat A. Diabetes, hypertension, and central obesity as cataract risk factors in a black population. The Barbados Eye Study. *Ophthalmology* 1999:**106**: 35-41.

84. Klein BE, Klein R, Lee KE. Diabetes, cardiovascular disease, selected cardiovascular disease risk factors, and the 5-year incidence of age-related cataract and progression of lens opacities: the Beaver Dam Eye Study. *Am J Ophthalmol* 1998:**126**: 782-790.

85. Reynolds A, Gallacher M, Fennerty C, Leyland M. Hospital management of cataract. *Optician* 2003:**225**.

86. Teikari JM, Virtamo J, Rautalahti M, Palmgren J, Liesto K, Heinonen OP. Long-term supplementation with alpha-tocopherol and beta-carotene and age-related cataract. *Acta Ophthalmol Scand* 1997:**75**: 634-640.

87. Meyer CH, Sekundo W. Nutritional supplementation to prevent cataract formation. *Developments In Ophthalmology* 2005:**38**: 103-119.

88. Asbell PA, Dualan I, Mindel J, Brocks D, Ahmad M, Epstein S. Age-related cataract. *Lancet* 2005:**365**: 599-609.

89. Rubin GS, Adamsons IA, Stark WJ. Comparison of acuity, contrast sensitivity, and disability glare before and after cataract surgery. *Arch Ophthalmol* 1993:**111**: 56-61.

90. Chylack L, Wolfe J, Singer D *et al.* The Lens Opacities Classification System III. *archives of Ophthalmology* 1993:**111**: 831-836.

91. Siik S, Chylack LTJr, Friend J *et al.* Lens autofluorescence and light scatter in relation to the lens opacities classification system, LOCS III. *Acta Ophthalmol Scand* 1999:**1999**: 5-509.

92. Sparrow JM, Bron AJ, Brown NA, Ayliffe W, Hill AR. The Oxford Clinical Cataract Classification and Grading System. *Int.Ophthalmol.* 1986:**9**: 207-225.

93. Sparrow NA, Frost NA, Pantelides EP, Laidlaw DA. Decimalization of The Oxford Clinical Cataract Classification and Grading System. *Ophthalmic Epidemiol* 2000:**7**: 49-60.

94. Maraini G, Rosmini F, Graziosi P *et al.* Influence of type and severity of pure forms of age-related cataract on visual acuity and contrast sensitivity. Italian American Cataract Study Group. *Investigative Ophthalmology and Visual Science* 1994:**35**: 262-267.

95. Stifter E, Sacu S, Benesch T, Weghaupt H. Impairment of Visual Acuity and Reading Performance and the Relationship with Cataract Type and Density. *Invest.Ophthalmol.Vis.Sci.* 2005:**46**: 2071-2075.

96. Elliot DB, Situ P. Visual acuity versus letter contrast sensitivity in early cataract. *Vision Research* 1998:**38**: 2047-2052.

97. Elliot DB, Hurst MA. Simple clinical techniques to evaluate visual function in patients with early cataract. *Optometry and Vision Science* 1990:**67**: 822-825.

98. Chylack LT, Jakubicz G, Rosner B *et al.* Contrast sensitivity and visual acuity in patients with early cataracts. *J Cataract Refract Surg* 1993:**19**: 399-404.

99. Chylack LT, Wolfe J, Friend J *et al.* Validation of methods for the assessment of cataract progression in the Roche European-American Anticataract Trial (REACT). *Opthalmol Epidemiol* 1995:**22**: 59-75.

100. van Rijn LJ, Nischler C, Gamer D *et al.* Measurement of stray light and glare: comparison of Nyktotest, Mesotest, stray light meter, and computer implemented stray light meter. *Br J Ophthalmol* 2005:**89**: 345-351.

101. Lasa MS, Datiles MB, III, Freidlin V. Potential vision tests in patients with cataracts. *Ophthalmology* 1995:**102**: 1007-1011.

102. van den Berg TJ, IJspeert JK. Clinical assessment of intraocular stray light. *Applied Optics* 1992:**31**: 3694-3696.

103. Meacock WR, Spalton DJ, Boyce J, Marshall J. The Effect of Posterior Capsule Opacification on Visual Function. *Investigative Ophthalmology & Visual Science* 2003:**44**: 4665-4669.

104. Elliot DB, Hurst MA, Weatherill J. Comparing clinical tests of visual loss in cataract patients using a quantification of forward light scatter. *Eye* 1991:**5**: 601-606.

105. Wegener A, Laser H. Image analysis and Sheimpflug photography of anterior segment of the eye. *Klin Monatsbl Augenheilkd* 2001:**218**: 67-77.

106. Masters BR. Three-dimensional microscopic tomographic imaging of the cataract in a human lens in vivo. *Optics Express* 1998:**3**: 332-338.

107. Moss I, Wild J. The influence of induced forward light scatter on the normal blue-on-yellow perimetric profile. *Graefes Arch Clin Exp Ophthalmol* 1994:**232**: 409-414.

108. Dengler-Harles M, Wild J, Cole M, O'Neill E, Crews S. The influence of forward light scatter on the visual field indices in glaucoma. *Graefes Arch Clin Exp Ophthalmol* 1990:**228**: 326-331.

109. Wood J, Wild J, Crews S. Induced intraocular light scatter and the sensitivity gradient of the normal visual field. *Graefes Arch Clin Exp Ophthalmol* 1987:**225**: 369-373.

110. Hudson C, Khanna CJ, Miller A, Gilmore E. A Method to Establish the Clinical Relevance of a Simulated Cataract Model. *The Journal of Ophthalmic Photography* 2003:**25**: 80-83.

111. Burke M, Khanna C, Miller A, Venkataraman S, Hudson C. The impact of artificial light scatter on scanning laser tomography. *Optom.Vis.Sci.* 2006:**83**: 222-227.

112. Bettelheim F, Siew E. Biological and physical basis of lens transparency. In: McDevitt D (ed) *Cell biology of the eye*. New York: Academic Press, 1982.

113. Gilmore ED, Hudson C, Venkataraman ST, Preiss D, Fisher J. Comparison of different hyperoxic paradigms to induce vasoconstriction: implications for the investigation of retinal vascular reactivity. *Invest Ophthalmol.Vis Sci* 2004:**45**: 3207-3212.

114. Venkataraman ST, Hudson C, Fisher JA, Flanagan JG. Novel methodology to comprehensively assess retinal arteriolar vascular reactivity to hypercapnia. *Microvasc.Res.* 2006:**72**: 101-107.

115. Guan, K, Hudson, C, Wong, T, Kisilevsky, M, Nrusimhadevara, RK, Lam, WC, Devenyi, RG, Mandelcorn, M, and Flanagan, JG. Retinal Hemodynamics and Systemic Measures in Stratified Groups of Diabetic Patients at Increasing Risk for the Development of Clinically Significant Diabetic Macular Edema. Invest.Ophthalmol.Vis.Sci. 45, E-Abstract 4081. 2004.

116. Hudson, C, Wong, T, Guan, K, Kisilevsky, M, Nrusimhadevara, RK, and Flanagan, JG. The relationship between change in visual acuity and the development of clinically significant diabetic macular edema (CSDME). Invest.Ophthalmol.Vis.Sci. 45, E-Abstract 4081. 2004.

117. Archer DB. Diabetic retinopathy: some cellular, molecular and therapeutic considerations. *Eye* 1999:**13**: 497-523.

118. Riva CE. Bidirectional LDV system for absolute measurement of blood speed in retinal vessels. *Applied Optics* 1979:**18**: 2301-2306.

119. Canon Inc. CLBF diameter reading system. Personal Communication. 6-2-2005.

120. Hubbard LD, Brothers RJ, King WN *et al.* Methods for evaluation of retinal microvascular abnormalities associated with hypertension/sclerosis in the Atherosclerosis Risk in Communities Study. *Ophthalmology* 1999:**106**: 2269-2280.

121. Wong TY, Klein R, Nieto FJ *et al.* Retinal microvascular abnormalities and 10-year cardiovascular mortality: a population-based case-control study. *Ophthalmology* 2003:**110**: 933-940.

122. Azizi B, Buehler H, Venkataraman S, Hudson C. Impact of simulated light scatter on the quantitative, noninvasive assessment of retinal arteriolar hemodynamics. *Journal of Biomedical Optics* 2007:**12**: 034021.

123. Elliott D, Bullimore M, Bailey I. Improving the reliability of the Pelli-Robson contrast sensitivity test. *Clin Vis Sci* 1991:**6**: 471-475.

Copyright Permission (Journal of Biomedical Optics)

From: Jane Lindelof (janel@spie.org)
To: Behrooz Azizi
Date: Wednesday, March 4, 2009 3:51:17 PM
Subject: RE: Permission to use

Dear Behrooz Azizi,

Thank you for contacting SPIE to request permission to reprint in your thesis the following paper and to reproduce its figures:

Impact of simulated light scatter on the quantitative, noninvasive assessment of retinal arteriolar hemodynamics
Behrooz Azizi, Heike Buehler, Subha T. Venkataraman, and Chris Hudson
J. Biomed. Opt. 12, 034021 (2007)

Publisher's permission is hereby granted under the following conditions: (1) the material to be used has appeared in our publication without credit or acknowledgment to another source; and (2) you credit the original SPIE publication. Include the authors' names, title of paper, volume title, SPIE volume number, and year of publication in your credit statement.

Please let me know if you have any questions or further requests.

Sincerely,

Ms. Jane Lindelof for
Eric Pepper, Director of Publications
SPIE
P.O. Box 10, Bellingham WA 98227-0010 USA
360/676-3290 (Pacific Time) eric@spie.org

Copyright Permission (Optometry Today)

From: David Challinor [mailto:davidchallinor@optometry.co.uk]
Sent: Tuesday, October 13, 2009 7:24 AM
To: Behrooz Azizi
Subject: Re: permission to use figures 8 and 9 from the following article: Optometry Today. 2001;41:26-30.

You need to use the following credit:

Reproduced by permission of OT, the magazine of the Association of Optometrists, www.optometry.co.uk

David Challinor
Editor OT

tel: 0207 202 8164
email: davidchallinor@optometry.co.uk
fax: 0207 202 8161

Copyright Permission (Canon Inc., Japan)

From: Morishige Kazunori [mailto: morishige.kazunori@canon.co.jp]
Sent: Friday, February 26, 2010 9:57 AM
To: Behrooz Azizi
Subject: Re: Copyright Permission

Dear Mr.Azizi,

Thank you for your information.

I confirmed your request with R&D group.
In conclusion, we give approval to you that you use our document.

Best Regards,
K.Morishige.

Kazunori Morishige
Technical Service Dept., Medical Equipment Group Canon Inc.
E-mail: morishige.kazunori@canon.co.jp
Tel: +81-3-3758-2111
Ex: 85870
Fax: +81-3-5482-3960

キヤノン株式会社
医療機器市場技術課
森重　和則　<morishige.kazunori@canon.co.jp>
〒146-8501
東京都大田区下丸子３－３０－２
TEL　：　03-3758-2111(代表）　内線（85848）H棟
FAX　：　03-3757-0287